J. Phys. B: At. Mol. Opt. Phys. 26 (1993) 561-598. Printed in the UK

TOPICAL REVIEW

Atoms in ultra-intense laser fields

K Burnett†, V C Reed† and P L Knight‡

† Clarendon Laboratory, Oxford University, Parks Road, Oxford OX1 3PU, UK
‡ Blackett Laboratory, Imperial College, London SW7 2BZ, UK

Abstract. The interaction of an atom with an ultra-intense radiation field is characterized by the involvement of many photons in absorptions and emissions. Of course the word 'intense' has to be compared with some atomic reference: if the induced transition coupling between bound states exceeds inherent widths, then the dressed atom Rabi oscillations which dominate the atomic evolution are typical intense field effects, even though laser intensities may actually be quite modest. When laser intensities exceed 10^{13} W cm^{-2}, and infrared frequencies are employed, then free electrons are dressed by interaction energies which exceed the photon energies. Non-perturbative continuum processes such as above-threshold ionization then occur, combined with the emission of very high order harmonics of the pump laser frequency. At higher laser intensities, the optical electric field can exceed the Coulombic binding electric field and allow over-the-barrier ionization, which defines a new regime of high intensity physics. In this region (or at higher intensities) the atomic electron charge cloud oscillates in the laser field with large amplitude excursions from the nucleus, during which time it is unable to absorb further photons. This stabilization regime is predicted to persist until the electron dressing energy approaches the rest-mass energy when wholly unexplored regions remain to be investigated.

In this topical review, we examine *theoretical* models of atoms dressed by intense fields. We review the breakdown of lowest-order perturbation theory and those 'essential states' methods adopted to include Rabi frequencies, Stark shifts, induced widths and continuum dressing. Newer methods more suitable for super-strong fields are described, such as Floquet and Volkov methods and the direct numerical integration of the Schrödinger equation. Such methods are used to provide completely non-perturbative strong field descriptions of atomic dynamics. We conclude with a brief examination of the relativistic effects expected to be important when new high intensity ultrashort pulse lasers currently under development are employed in strong field physics.

1. Introduction

Prior to the production of intense coherent radiation from lasers, Einstein's law for the photoelectric effect adequately described the ionization of matter under the influence of light. This law, justified formally by lowest order perturbation theory and Fermi's golden rule, is strictly concerned with the absorption of a single photon during a transition from a discrete level to a continuum and was formulated before light sources were available that were intense enough to produce multiphoton effects.

Multiphoton transitions were first predicted by Göppert-Mayer in 1931 [1] and observed at radio frequencies by Hughes and Grabner in 1950 [2]. The study of multiphoton absorption at optical frequencies only became possible when intense laser sources were developed. Following this, in 1961, Kaiser and Garret observed two-photon absorption in a crystal [3] and Abella observed such absorption in caesium atoms in 1963 [4]. Multiphoton ionization (MPI) was first observed in the experiments

0953-4075/93/040561+38$07.50

of Hall, Robinson and Branscomb, in which a ruby laser was used to induce two-photon detachment from negative halogen ions [5]. Later, MPI from rare gas atoms was observed by Voronov and Delone [6] and Agostini *et al* [7].

Multiphoton free-free transitions were first observed in 1977 by Weingartshofer *et al* who studied multiphoton absorption and emission in laser-stimulated electron scattering [8]. Later experiments by Agostini *et al* measuring the energy of the photoelectrons produced by the MPI process revealed that free-free transitions can accompany MPI, when electrons absorbed additional photons, more than was required for ionization [9]. This phenomenon has become known as above-threshold ionization (ATI) and many experiments have been performed to study it, using wavelengths from 10 μm to 250 nm, intensities up to 10^{18} W cm^{-2} and pulse lengths from hundreds of picoseconds down to a fraction of a picosecond [10]. It was suggested by Shore and Knight in 1987 that the coherent excitation of highly energetic continuum states could allow the generation of extremely high harmonics of the laser field [11]. Such harmonic spectra have been observed experimentally up to high order in high intensity lasers: the 53rd harmonic of 1053 nm light in neon [2, 13], and the 45th harmonic of 527 nm light [14] and the 41st harmonic of 616 nm light in helium [15]. The two shortest wavelengths yet produced are the 25th harmonic of 248 nm light in helium [16] and the 109th harmonic of 806 nm light in neon [17]. These harmonics are of particular interest as a possible source of coherent x-ray radiation.

With the experimentally obtainable intensities continually increasing because of developments in short-pulse laser physics, recent interest has focused on the possibility of atoms surviving in pulses of intensities of the order of 10^{20} W cm^2, with lifetimes that *increase* with increasing intensity. Various possible mechanisms have been suggested that could bring about this ionization suppression, and recently the first experimental observations of ionization suppression have been reported, involving the formation of an extended wavepacket of bound states that has little overlap with the nucleus and hence a low ionization rate.

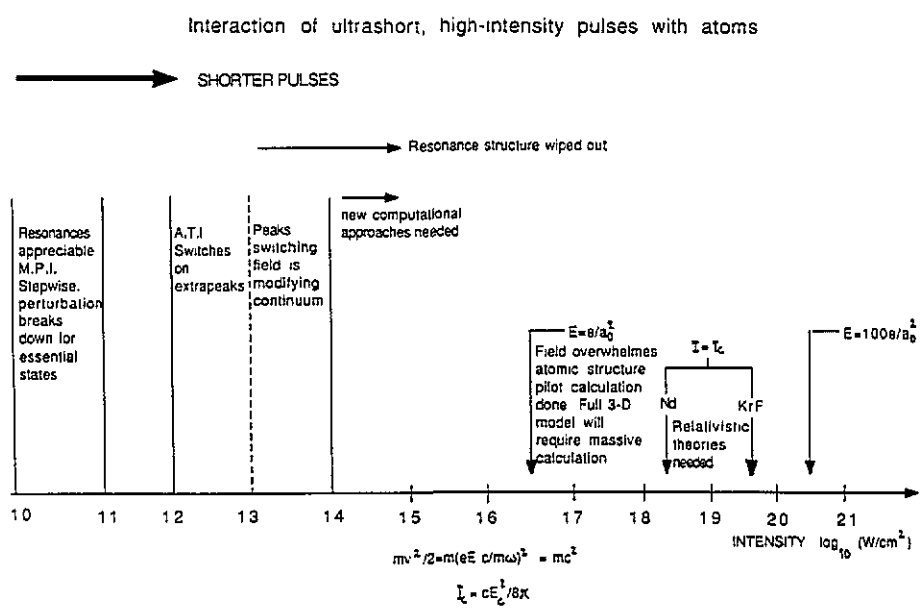

Figure 1. Schematic diagram showing the various interaction regions of an atom with an ultrashort high intensity laser pulse.

In this article, these various aspects of multiphoton behaviour in ultra-intense fields will be studied: by ultra-intense, we mean fields where the laser–atom interaction is too large for even many-order perturbation theory to be valid, which implies laser intensities above approximately 10^{13} W cm^{-2}. To illustrate this, in figure 1 we give a schematic representation of the various interaction regions of an atom with an intense laser field.

2. Photoelectron spectra

High energy photoelectrons produced by multiphoton ionization were first reported by Martin and Mandel [18], and Boreham and Luther-Davies [19]. One of the first observations of a well resolved ATI spectrum was reported by Agostini *et al* [9]. Using the second harmonic of a Nd-glass laser with a wavelength of 532 nm, and a peak intensity of 8×10^{12} W cm^{-2}, Agostini *et al* observed an extra peak in the photoelectron spectrum. The peaks were separated by the photon energy, with the higher energy peak having a height of approximately ten times less than the lower energy one. Since this early experiment, ATI spectra consisting of many peaks have been observed in many different atoms and molecules, using lasers of a wide variety of wavelengths, from infrared to ultraviolet.

By the early 1980s, the sophistication of ATI experiments had improved, with the introduction of electron spectrometers with a wider acceptance angle and higher resolution. The photoelectron spectra produced showed several ATI peaks at lower intensities than previously used [20, 21]. These early experiments, of which that performed by Kruit *et al* is a good example, produced a typical ATI spectrum consisting of multiple peaks, separated by the photon energy (figure 2) [22]. The number of these peaks was seen to increase with intensity and their positions in the photoelectron energy spectrum were accurately given by the formula

$$E = E_g^{(0)} + n\hbar\omega \tag{1}$$

where $E_g^{(0)}$ is the field-free ground state energy and n is the number of photons absorbed.

It can be seen from figure 2 that the positions of the peaks in the energy spectrum are independent of intensity, but that as the intensity increases, the lowest order peak is reduced in magnitude and vanishes for the highest intensity shown. The reason for this peak suppression, also reported in the experiments of Muller *et al* [23], lies in the shifts of the atomic states induced by the laser field. When a free electron is in a laser field, it possesses a kinetic energy due to its oscillation in the laser field. The cycle-averaged kinetic energy, the so-called ponderomotive energy, E_p, is given by the expression

$$E_p = \frac{e^2 \mathscr{E}_0^2}{4 m_e \omega^2} \tag{2}$$

where $\mathscr{E}_0$ is the local peak electric field, ω is the angular frequency of the laser and e and m_e are the electron's charge and mass respectively. The total energy of a free electron becomes the sum of the ponderomotive energy and the translational energy:

$$E_{\text{total}} = E_p + \tfrac{1}{2} m_e \langle v \rangle^2 \tag{3}$$

where $\langle v \rangle$ is the average velocity over one cycle. High intensity fields also have an effect on the bound electrons and all the energy levels of the atom are shifted to some

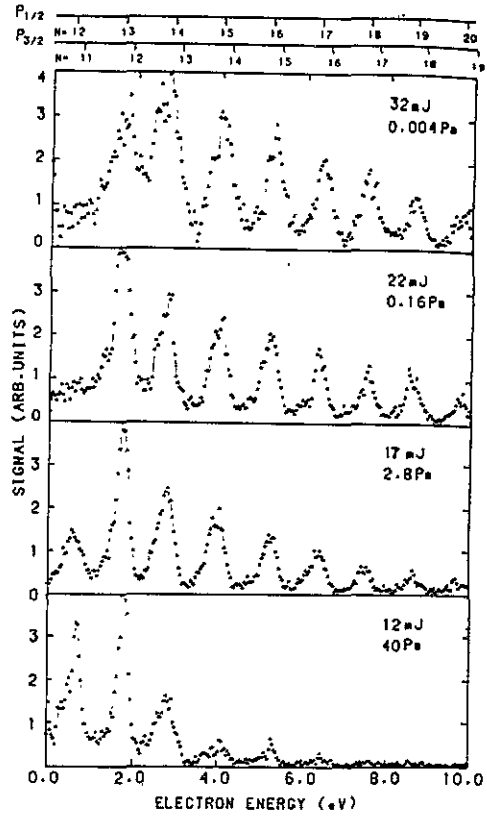

Figure 2. Photoelectron spectra from xenon using a 1064 nm laser with intensities given by the expression $I = F \times 10^{12}$ W cm^{-2}, where F is the photon energy (mJ) [22].

extent: this is the AC Stark shift. Because the binding energies of the Rydberg states are small, their induced shifts are essentially given by the ponderomotive energy. One can visualize this by considering that the nucleus only restrains the free oscillation of the bound electron by a small amount. However, deeply bound states can only oscillate slightly in the stronger nuclear field compared to the Rydberg and continuum states and so their shifts are small. Typical values for free electron ponderomotive shifts in a 10^{13} W cm^{-2}, 1064 nm Nd:YAG laser are 1.06 eV, compared with a shift of 0.008 eV for the ground state in hydrogen [10]. Therefore the Rydberg and continuum states shift upwards, relative to the lower bound states, by approximately E_p and produce an increase in ionization threshold, given approximately by the ponderomotive shift [24]. When this threshold shift is large enough so that

$$E_g^{(0)} + n\hbar\omega \geq 0 \tag{4}$$

but

$$E_g^{(0)} + n\hbar\omega - E_p \leq 0 \tag{5}$$

then the channel for n-photon absorption is closed and the peak in the ATI spectrum is suppressed. Of course in a smoothly varying pulse, the channel may not be closed for the whole duration of the pulse and so the peak will not be completely absent.

Channel closing has been studied in detail experimentally: Lompré *et al* have observed the closing of up to three channels in helium at 4.42×10^{13} W cm^{-2} using 532 nm light [25]. Recently, using longer wavelength light of 10.6 μm from a 10^{13} W cm^{-2} CO_2 laser, Xiong *et al* have reported hundreds of missing peaks in xenon [26].

If there is an intensity-dependent shift in the ionization threshold of the atom, the question then remains as to why the ATI peak positions, as shown in figure 2, are not intensity-dependent in long laser pulses. Bucksbaum *et al* address this question and discuss how an electron gains an amount of energy equal to the ponderomotive energy as it leaves the focus of the laser beam [27]. This increase in energy approximately cancels out the decrease in the nascent energy of the electron due to the increase in ionization threshold and so the electron detector does not measure any energy shift from the ATI peak positions predicted by equation (1). Consider the kinetic energy of the electron in the beam: if we write electron's velocity in two parts, translational and oscillatory, v_t and v_o, then we can write its kinetic energy as

$$E_{KE}=\tfrac{1}{2}m_e\langle v_t\rangle^2+\tfrac{1}{2}m_e\langle v_o\rangle^2. \tag{6}$$

We can then consider the second term in this expression, which represents the ponderomotive energy of the electron, as defining a ponderomotive potential down which the electron passes as it moves out of the edge of the laser beam. The ponderomotive energy of the electron is then transferred to its translational energy and the energy measured at the detector outside the laser beam is now correctly predicted by equation (1). Bucksbaum *et al* describe this process as 'surfing'. The electron is accelerated in the direction of the steepest gradient of the ponderomotive potential, ∇E_p, and because the ponderomotive energy can be large, the detected energy can be many times more than the nascent energy of the photoelectron and the direction in which it is detected can bear little resemblance to the direction of its original trajectory, which is peaked in the direction of the electric field polarization [27, 28].

Typically an electron will take a few picoseconds to leave the focus of a laser in a typical ATI experiment [10]. If the pulse length is significantly greater than this time, then all the ionized electrons have sufficient time to pass out of the edge of the beam and the detected photoelectrons have energies given by equation (1). If the pulse length is decreased to around 50 ps, the ATI peaks begin to smear, because not all of the electrons have enough time to travel down the ponderomotive potential and out of the edge of the beam before the pulse is passed and some of the electrons only acquire part of the ponderomotive energy [29]. In very short pulses, less than a picosecond, the pulse passes by the electron before it can travel any appreciable distance and be accelerated by the ponderomotive potential. What is recorded at the detector therefore is the nascent energy of the electrons that was acquired during the ionization process: hence a short pulse brings about a red shift in the ATI peaks. In Petite *et al*'s experiment, it is noticeable that these red shifts are greater for the lower energy peaks, because, having less energy, these electrons do not pass so far towards the edge of the beam and so acquire a smaller proportion of the ponderomotive energy [29].

In order to examine the nascent energy spectrum in an ATI experiment, we must therefore use very short pulses. Using a long pulse masks any resonance effects, because no matter at what intensity in the pulse an electron is ionized, the decrease in its free electron energy value due to the shifting ionization potential is compensated for by the acceleration due to the ponderomotive potential. In short pulses however, the ATI peaks split into series of fine peaks, which can be partly interpreted in terms of bound state resonances [30, 31].

Most of the early work on multiphoton ionization examined the number of ions produced by an MPI process, which was found to be proportional to I^n, where n is the number of photons absorbed and I is the field intensity, in accordance with the prediction of perturbation theory. However this intensity scaling breaks down at some critical intensity, I_s, above which there was a marked change in the intensity dependence. Lompré *et al* observed such a breakdown for xenon, helium and neon at around 10^{13} W cm^{-2} from a 5 ps, 1064 nm Nd:YAG laser pulse [25].

This phenomenon is explained in terms of population depletion. For any pulse of long enough pulse length and high enough intensity, there is a maximum value of the intensity beyond which no more ionization will take place, because all the atoms in the interaction volume, in this case the laser focus, are ionized. This intensity is known as the saturation intensity, I_s, and the intensity in the ion production graphs at which the gradient ceases to be a straight line. If the peak intensity of the pulse is above this intensity, ionization only takes place at the beginning of the pulse.

Above this saturation intensity, expansion of the effective interaction volume occurs. As the intensity is raised, the intensity in the region outside the focus becomes sufficiently large to make a noticeable contribution to the ionization rate. If such an expansion did not occur, then the graph of number of ions against intensity on a logarithmic plot would become horizontal above the saturation ionization instead of the slow increase that is observed. The rate of ionization is no longer governed by the n-photon ionization process, but instead depends on the geometric properties of the lens.

Studying the photoelectron spectra from atoms irradiated by an intense laser field is a useful means of obtaining information about the multiphoton processes taking place. Such spectra can given an indication as to when the use of perturbation theory is no longer valid, because at higher intensities, above approximately 10^{13} W cm^{-2}, the shape of the envelope of the ATI peaks changes. The lowest order ATI peak is no longer the largest peak, indicating that higher order multiphoton processes can dominate the interaction, in direct contradiction to the basic assumptions of perturbation theory [25, 32].

Various characteristics of the photoelectron spectrum have been studied and are reasonably well understood. In short pulses, bound state resonances can produce identifiable peaks in the ATI spectrum as the time varying pulse sweeps different states into multiphoton resonance by the action of the time-dependent Stark shift. The time-varying pulse can also cause a 'fringe' pattern in the photoelectron spectrum as the ionization from the rising and falling edge of the pulse interferes [33]. This quantum interference has been identified in theoretical calculations, but will be harder to observe experimentally because of the smearing of the pattern due to spatial extent of the laser beam.

The origins of the substructure in the photoelectron spectrum at intensities lower than around 10^{14} W cm^{-2} have been extensively studied, as outlined above. However, at higher intensities, results show that the general shape of the ATI spectrum can considerably change, with the pattern of the ATI peaks no longer being discernible [34]. This loss of regular structure can be interpreted qualitatively by considering the ionization process that occurs at these high intensities. Although it is rather a quasistatic picture, one can imagine that above a certain critical intensity, of the order of 1.4×10^{14} W cm^{-2} in hydrogen, ionization can take place by the electron wavepacket passing directly over the resultant potential barrier of the instantaneous incident electric field and atomic potential: this has been termed as over-the-barrier (OTB) or barrier-

suppression ionization [34, 35]. This fast ionization process destroys the regular pattern that would otherwise occur in the photoelectron spectrum and the ionized wavepacket is scattered by the nucleus as it moves away, resulting in the apparently random structure that is observable. This is further discussed below and in [34].

Further complications in comparing theoretical and experimental photoelectron spectra arise from the fact that most experimental targets are multielectron atoms and therefore the observed spectra may be produced by electrons ejected from different stages of ionization: typically Xe^{3+} can be produced in a 1 ps, 5×10^{14} W cm^{-2}, 1064 nm pulse [35, 36]. As yet there are few reported experiments using atomic hydrogen as the target, but recent experimental results using linearly polarized light at 608 nm and at intensities of either 6 or 12×10^{13} W cm^{-2} have been compared with theoretical Floquet-based results. There is good agreement for the relative subpeak heights and spacings, but the relative ATI peak heights are not adequately represented. There are experimental peaks not reproduced in the theory and there is considerably more experimental background particularly at the higher intensity [37]. We will discuss this further below.

3. Theoretical treatments of multiphoton interactions

3.1. The breakdown of perturbation theory

Multiphoton ionization at relatively low intensities ($<10^{13}$ W cm^{-2}) can be described by perturbation theory applied to a bound-free transition. Many-order perturbation theory may be necessary, because many photons may be absorbed during the ionization process. Further absorption of photons in the continuum may also take place, forming the higher energy ATI peaks [38–40]. Perturbation theory predicts that the ionization rate for an n-photon ionization process has the following power law dependence on intensity:

$$\frac{\mathrm{d}P_n}{\mathrm{d}t}\propto I^n \tag{7}$$

where P_n is the ionization probability. This relationship is difficult to test accurately, because of the pulsed focused laser beam that is used, which has varying intensity in time and across the beam profile [10]. However, experiments have been performed that find significant discrepancies from the perturbation theory power law [20–22, 41]; these discrepancies signal the breakdown in perturbation theory. The first sign of a breakdown of lowest order perturbation theory which underlies equation 7 is that energy levels can be Stark shifted by large amounts from their unperturbed positions and broadened by the stimulated transition rates to other levels. This leads to intensity-dependent corrections to the multiphoton absorption generalised cross sections. When population can be resonantly excited out of initial bound states, the consequent depletion clearly violates the basic assumption of perturbation theory. Indeed population can be periodically transferred between resonant levels in multiphoton Rabi oscillations and the whole concept of a time-dependent rate of ionization becomes meaningless. These topics, of central concern to the field a decade or more ago, are clearly reviewed in articles by Lambropoulos, and Georges and Lambropoulos [42]. At greater intensities, ($>10^{13}$ W cm^{-2}), the whole idea of perturbation theory breaks

down and an alternative non-perturbative procedure must be used. To illustrate this, consider the expansion of the polarization, P, of an atom in an incident electric field [43]:

$$P = \varepsilon_0\chi_1\mathscr{E} + \varepsilon_0\chi_2\mathscr{E}^2 + \varepsilon_0\chi_3\mathscr{E}^3 + \ldots \tag{8}$$

where χ_i is the ith-order susceptibility. The ratio of successive terms may be estimated as

$$\frac{\varepsilon_0\chi_{i+1}\mathscr{E}^{i+1}}{\varepsilon\chi_i\mathscr{E}^i} \approx \frac{\mathscr{E}d}{\Delta} \tag{9}$$

where d is a typical dipole matrix transition element, ($d \sim ea_0 \sim 10^{-29}$ C m), and Δ is the energy detuning of the incident laser from a resonance line of the atom (typically 0.5 eV). It can be seen that for intensities greater than approximately 10^{13} W cm^{-2}, this ratio is greater than one and the series is divergent.

Non-perturbative calculations are inherently difficult because no analytical solutions of the Schrödinger equation of an atom in a time-varying electric field are known except for the δ-function potential [44]. Various non-perturbative approaches have been developed and we shall be giving a brief overview of them in the next section. Such calculations are generally only concerned with single atoms in plane wave fields. Ponderomotive effects that act on the electrons as they leave the beam focus are not easily included and therefore these calculations are more commonly applied to multiphoton processes in the short pulse regime. When studying the resonance structure in the spectra from short pulses, it is important to consider the temporal and spatial intensity variations of the laser pulse, because a measured photoelectron spectrum represents some average of the single atom spectra from the atoms exposed to different intensities across the beam. Phase fluctuations in a pulse of large bandwidth can also significantly smear the photoelectron spectrum. In general only rather crude characteristics of the pulse in space and time can be obtained. This makes direct quantitative comparisons with theory rather difficult [10]. However theoretical results can shed light on the underlying physical processes and can provide indications of the directions that experimental investigations should take and hence significantly enhance the understanding of multiphoton ionization.

3.2. Non-perturbative theoretical calculations

Perhaps the most straightforward method of non-perturbative calculation is the direct time integration of the Schrödinger equation. With the aid of an infinitely fast computer, it would be possible to calculate accurately the behaviour of a many-electron atom in an intense laser field. However, at present it is beyond the means of computers to calculate the photoelectron spectrum even of hydrogen in a realistic length pulse of 1 picosecond. The reason for this lies in the continuum–continuum transitions that occur when the higher above-threshold (ATI) peaks of the photoelectron spectrum are formed. These continuum–continuum transitions produce high energy electrons that rapidly move away from the atomic core. Because of the large distances that such electrons travel in a realistic length pulse, the grid on which the calculation is performed must be large, so that the high energy electron wavepackets never reach the edge of the grid. Such large grids require impossibly large amounts of computer time. To illustrate this, consider a circularly polarized laser pulse of wavelength 532 nm and pulse length 1 ps. Suppose that the 4th ATI peak is visible, then this peak will have an energy of order four times the photon energy ($4 \times 0.086 = 0.344$ au), corresponding to a velocity of

0.829 au. In 1 ps (41 322 au), this wavepacket can travel $0.829 \times 41\,322 = 34\,256$ au towards the edge of the grid. Making a conservative estimate of 0.2 au for the spacing between the grid points this would mean a three-dimensional grid would need $(34\,256 \times 2/0.2)^3 \approx 10^{16}$ points! This is prohibitively large. This has restricted direct three-dimensional integrations to pulse lengths of approximately 50 fs and intensities below around 5×10^{15} W cm^{-2}, although such calculations are still very considerable computational achievements.

To avoid the need for excessive amounts of computer time, several other theoretical approaches have been developed. Various approximations have been applied to direct time-integration methods and alternative theoretical treatments have been used. We will next consider some of these in detail.

3.3. Essential states methods

Various non-perturbative calculations have been carried out which specifically include continuum–continuum transitions, which redistribute the population in the continuum [45–48]. The most straightforward of these modelled the atom by a single bound state and various continua, each corresponding to a particular angular momentum [48, 49]. Non-resonant MPI takes place into a continuum and further photon absorption transfers population into the other continua. The wavefunction at any time is written in terms of the single bound and various continuum wavefunctions and the various states are connected by (usually dipole interaction) matrix elements. The actual calculation involves the solution of the set of coupled equations to obtain the populations of the various states. Such a method has successfully demonstrated the importance of continuum–continuum transitions and has predicted the onset of peak saturation, where the higher energy ATI peaks have a greater magnitude than the lower ones, i.e. 'peak switching' [48, 49]. However, all these calculations face the same restriction that the theories are unable to make quantitative predictions for the spectra to compare with experiments, partly because the transition matrix elements for the complex atoms used in the experiments are not known. Also many states, including the various angular momentum states in the continuum may have to be considered to allow for all possible transitions. One further difficulty lies in the fact that multiphoton coupling between continuum states must be included as well as single photon coupling and in fact these couplings can often be singular [50, 51].

This type of calculation uses what is known as the essential states method. Originally the essential states which were employed were those of the unperturbed atom, but as the laser intensity increased, the number of states which are necessary for converged solutions grows too large for this method to be practical. Other calculations following the same principles, but including very many states are those of the type performed by Tang *et al* [52] and other authors [53, 54]. In these calculations, the hydrogenic wavefunctions are expanded in terms of selected states from some complete set of wavefunctions, e.g. Sturmian basis set or B-spline functions, which have the effect of discretizing the continuum in one form of the other. The Schrödinger equation then reduces to a set of differential equations relating the coefficients of these functions, which are solved numerically.

When continuum–continuum transition amplitudes are small (i.e. for high frequencies and not too high intensities), the conventional essential states method can be employed profitably to study bound state excitation, Rydberg state wavepacket formation, dynamic Stark-induced resonances and the like. For example, Piraux and Knight

[55] use an essential states method to study the role of the counter-rotating terms in photoionization. Essential states methods, involving very many bound states, have also been used by Fedorov and Movsesian and others [56], Parker and Stroud [57] and Piraux *et al* [58] to study ionization suppression and population trapping in Rydberg atoms. In the paper of Piraux *et al* an essential states method was employed to describe one- and two-photon ionization of atomic hydrogen by an ultra-short hyperbolic secant laser pulse. The method used a Coulomb Green function to include all atomic state contributions (in the rotating-wave approximation) to Stark and Raman coupling terms, and care was taken to include sufficient bound states to ensure convergence. They considered two frequency regimes. For photon energies close to the ionization potential, they showed that the excitation of atomic hydrogen, initially in its ground state leads, at low and moderate laser intensities, to an np state population distribution, which is strongly shifted down to low lying Rydberg states for ultra-short pulses. At very high intensities in this frequency regime, they showed that the time evolution of the Rydberg state population follows adiabatically the pulse shape and does not lead to population trapping in the Rydberg states. They also demonstrated for two-photon ionization that there is significant inhibition of ionization at high field intensities. The stabilization is caused by the creation of a spatially extended wavepacket, produced by the Raman mixing of intermediate Rydberg states; we will discuss this further in section 5.1.

3.4. Volkov final state theories

The Schrodinger equation for a free electron in a plane wave electric field, but outside the range of the atomic potential is exactly solvable. The solutions, known as Volkov states, are plane waves with an oscillating phase, which depends on the vector potential. When the dipole approximation is valid, these solutions may be written as

$$\phi_v(\boldsymbol{r}, t) = \exp\left(\frac{\mathrm{i}}{\hbar}[\boldsymbol{p} - e\boldsymbol{A}(t)] \cdot \boldsymbol{r} - \frac{\mathrm{i}}{\hbar}\int_0^t \frac{1}{2m}[\boldsymbol{p} - e\boldsymbol{A}(\tau)]^2 \,\mathrm{d}\tau\right). \tag{10}$$

Here $\boldsymbol{p}$ is the electron's momentum [59].

Calculations can be performed by assuming that an ionizing electron makes a transition between two well defined states: the initial bound Coulombic wavefunction and the final free-electron Volkov solution. Keldysh used this approach to examine tunnelling ionization [59] and following on from this work a wide range of similar non-perturbative calculations have been performed, led predominantly by Faisal [60] and Reiss [61-63]: these are collectively known as the KRF models. Following Keldysh, the KRF models use Volkov states as approximations to the final state of the electron, field-free eigenstates as initial wavefunctions and connect the states by some interaction. The system wavefunction is written in terms of the bound states of the atom and Volkov functions, and the evolution of the system is described in terms of a set of coupled, first-order differential equations, whose solution is the time-dependent expansion coefficients of the bound and Volkov states. However, such calculations implicitly neglect the laser-induced level shifts and the effect of the ion on the electron as it ionizes and passes out of the region of the atomic potential. Also this approximation is really only valid if the system is not appreciably ionized. Furthermore, there is an upper limit to the intensity for which this approach is valid because when the ponderomotive energy of the electron is larger than the binding energy of the atom, then the initial state of the atom can no longer be taken as an unperturbed eigenstate.

There has been extensive work performed using Keldysh theory as a basis, examining such aspects as the role of the Volkov states on the ATI spectra obtained [64, 65] and the role of the ponderomotive shift on the ATI peak positions [66, 67]. Further extensions to the theory have included the use of an effective multiphoton matrix element that lifts the electron into the continuum with the minimum number of photons and then considers transitions between Volkov states, forming the higher ATI peaks [64, 65] and the role of the Coulomb interaction on the final states [68].

However even without these refinements, Keldysh theory has produced results that show quite good agreement with the photoelectron spectra from xenon, krypton and helium, illuminated with circularly polarized light for long pulses for which it is expected that the effect of bound state resonances will be minimal [62, 69]. The agreement of KRF theory with experiment for linearly polarized light is much poorer. This has been attributed to the fact that lower angular momentum electrons are produced which penetrate the atomic potential more and so the Volkov approximation is less valid [70]. Further calculations to predict the angular distribution of the ejected electrons from atoms illuminated by elliptically polarized light show fair agreement [68, 71]. However there are limitations to this type of approach and the theory will not be valid when the pulse length is short enough for the intermediate resonances to become important [10], or the depletion from the initial state becomes significant.

3.5. Floquet theory

Recently there has been much effort focused on the Floquet method of finding solutions to the Schrödinger equation of an atom in an intense laser field. One of the first applications of Floquet theory to atomic systems was made by Shirley [72]. He used the technique to replace the semiclassical Hamiltonian of a quantum system in an oscillating field with a time-independent Hamiltonian represented by an inifinite matrix. The formulation of Floquet theory starts with the Schrödinger equation

$$i\hbar \frac{\partial |\phi(t)\rangle}{\partial t} = H(t)|\phi(t)\rangle \tag{11}$$

with the Hamiltonian $H(t)$ written in the form

$$H(t) = \left(\frac{p^2}{2m} + V(r)\right) + H_1(t) \tag{12}$$

where $V(r)$ is the atomic potential and $H_1(t)$ is the laser interaction term, which can be written as

$$H_1(t) = H_+ e^{-i\omega t} + H_- e^{i\omega t}. \tag{13}$$

When the Hamiltonian of a system is periodic, such that $H(t+\tau) = H(t)$, then the Floquet theorem can be used to write the wavefunction in the form

$$|\phi(t)\rangle = e^{-iEt/\hbar}|F(t)\rangle. \tag{14}$$

The Floquet theorem asserts that the Floquet vector $|F(t)\rangle$ is also periodic with the same period as the laser field in t; it can therefore be expressed in the form

$$|F(t)\rangle = \sum_n e^{-in\omega t}|F_n\rangle. \tag{15}$$

We can consider this as indicating that the nth harmonic component represents an electron which has absorbed n photons. Inserting the Floquet vector $|F(t)\rangle$ into the Schrödinger equation produces an infinite set of coupled algebraic equations

$$[E + n\hbar\omega - H_a]|F_n\rangle = V_+|F_{n-1}\rangle + V_-|F_{n+1}\rangle. \tag{16}$$

This system of coupled equations is manifestly time independent and has solutions with complex quasi-energies that represent decaying states. The complex Floquet quasi-energy that is obtained from the solution of these equations can be written as

$$E = E_0 + \Delta - i\Gamma/2 \tag{17}$$

where E_0 is the unperturbed energy of the state, Δ is the Stark shift and Γ is the width of the state and represents the ionization rate [73].

Using such a construction, multiphoton ionization rates and threshold shifts have been obtained [74] and recently important calculations have been performed by Shakeshaft and co-workers to examine the role of resonances on the ionization rate and photoelectron spectra of atomic hydrogen [75]. In these calculations, values for the ionization rates, angular distributions and Stark shifts of the hydrogen atom in monochromatic laser fields were obtained. The technique relies on using the Floquet expansion to obtain an infinite series of coupled equations, connecting the harmonic components of the Floquet expansion of the wavefunction. The harmonic components are composed of a discrete complex Sturmian basis set. Particularly interesting results from this work have been the observation of multiphoton resonance enhancement in MPI and the interpretation of the photoelectron peaks due to these resonances. Potvliege and Shakeshaft have been able to compare their predictions for the positions of the resonance peaks in the photoelectron spectrum from atomic hydrogen with data obtained from experiments on hydrogen performed at the University of Bielefeld [76] by Feldmann and co-workers. The Floquet calculations show good agreement with the lowest energy peak in the spectrum in many respects, although there is some structure that is unexplained, as mentioned above. However, what is not fully accounted for in these calculations is the full time dependence of the incident laser pulse, because the calculations only contain a purely monochromatic electric field. The effects of pulsed fields are therefore constructed from a sequence of constant envelope calculations and some features of the dynamics in a real pulse are therefore not represented. Also these calculations cannot easily describe the high energy photoelectron peaks, nor calculate peaks at high intensities significantly above 10^{14} W cm^{-2} because of the size of calculation involved. (The size of the calculation increases rapidly with the number of channels in the Floquet expansion.)

Another major application of Floquet theory exploits the R-matrix technique of electronic collisions combined with the Floquet method for the applied laser field. This approach, when fully implemented computationally, will be a powerful tool for examining a wide range of systems in laser fields [77].

3.6. Direct integration of the Schrödinger equation

The final approach that has been extensively used to study MPI is that of the direct numerical integration of the time-dependent Schrödinger equation. As was reported above, the complete solution of the three-dimensional Schrödinger equation in a realistic time-dependent laser pulse is not at present computationally possible so such numerical studies use various different approaches to reduce the computation time

required. Perhaps the most straightforward method of reducing the amount of computation needed to perform these calculations is only to consider one dimension. This approach has been taken by several workers [33, 78–82] and such calculations have produced many results that have contributed much to the understanding of multiphoton processes. Such one-dimensional calculations represent an extreme simplification of actual experimental conditions: the beam has no transverse structure, the magnetic field is neglected [83] and the Coulomb potential must be replaced by some model potential [33, 78–80, 82, 84–89].

The advantages of the one-dimensional calculations are many. They are relatively fast, allowing many calculations to be performed to study the effect of varying parameters on the multiphoton ionization process: for example, ATI spectra can be studied as a function of angular frequency, intensity or pulse length. The photoelectron and harmonic spectra from realistic length pulses can be calculated, which is impossible in three dimensions because of the excessively long calculation time that this would take. Fine detail in the plots of ionization as a function of time can be produced, which can shed much light on the physical processes: this is not possible in three dimensions. Because of the ease of computation, one-dimensional calculations have also been used to test other calculational approaches, Javanainen and Eberly [90] compared various Keldysh calculations with one-dimensional calculations, and Pindzola and Dörr [91], and Bardsley *et al* [80] have compared Floquet calculations with *ab initio* numerical calculations for smooth pulses.

Three-dimensional calculations are, of course, more realistic, but represent a far more formidable computing task. To reduce the size of the calculation, only linearly polarized light is usually considered, so that the system has axial symmetry in the dipole approximation and the dimensions considered can be reduced by one. Such three-dimensional calculations have been performed by Kulander and co-workers and they have been used to study, for example, the effect of bound state resonances on harmonic spectra [92, 93].

Various calculations have also been performed in three dimensions for multielectron atoms [92–95]. For example, Kulander used a time-dependent Hartree–Fock model, or frozen core model, to calculate ionization rates and wavefunctions of helium and neon for approximately ten cycles of the laser field. Such calculations are extremely difficult because the electrons experience interelectron forces, and the number of points on the grid of the calculation must be large. Single-atom harmonic spectra from xenon have also been studied, for pulses up to twenty cycles long. Such spectra have been compared to those obtained experimentally and whilst the pulse lengths in the three-dimensional calculation are of course considerably smaller than those obtained experimentally, the spectra do exhibit resonances and plateaux, which are qualitatively comparable with experiments [96, 97].

Another approach to three-dimensional calculations has been adopted by LaGatutta [98], Sanpera and Roso-Franco [99], DeVries [100] and Krause *et al* [101]. The wavefunction is expanded in spherical harmonics, resulting in a series of coupled equations relating the coefficients of the various angular momentum states. In the length gauge for a linearly polarized field, the coupled equations relating the coefficients of these harmonics only contain coupling terms between the coefficients of states whose angular momentum differs by one: thus the equations become relatively easy to solve. In spite of this, such a calculation is still at least of the order of L times slower than one-dimensional calculations, where L is the total number of angular momentum states considered, of the order of 10. So only very short pulses have been studied, of a few

laser cycles in length. For example, Krause *et al* have calculated the harmonic spectra from 20 cycle laser pulses.

Finally, classical calculations have been performed to study MPI, usually relying on Monte Carlo techniques to follow the electron trajectory. The technique follows the time evolution of an initial three-dimensional microcanonical distribution, associated with ground-state hydrogen atoms. This method, sometimes known as the phase space averaging method [102–104], begins by obtaining the initial conditions of very many electronic trajectories by simulating the statistical distribution characteristics of the initial wavefunction. Each trajectory is then calculated using classical dynamics and then the properties of the summation of these trajectories are examined. Many such calculations have been performed, examining photoelectron spectra [105, 106], electron trajectories [106, 107], harmonic generation [108] and atomic stabilization [109] from both ground state and Rydberg atoms. Classical calculations have been performed, investigating the ionization of highly excited atoms in microwave fields. These calculations have observed certain classes of trajectories that do not ionize. These trajectories have been linked with the appearance of anomalously stable states in the microwave ionization experiments of Sauer *et al* [110], and are associated with the production of 'scars' in classically chaotic systems [111].

To conclude this section we should note that the multiphoton ionization process is very complex and no one type of calculation models all the relevant aspects. So although all the above calculational techniques that directly integrate the Schrödinger equation rely on some approximation to make finding the solution easier, they can all provide important insight into the multiphoton ionization process.

4. The generation of harmonic spectra

In 1987, Shore and Knight pointed out that high-order odd-harmonic generation could take place by the emission of a high energy photon from a transition between a high energy continuum state and a low lying bound state [11]. Previous to this, relatively low-order harmonic generation had been reported due to predominantly bound state multiphoton transitions (although Miles and Harris and others exploited autoionizing continuum resonances to enhance the production of harmonics). When ATI populates high energy continuum states, very high-order harmonic processes can occur [112].

One of the first experiments in which these high order harmonics were observed was performed by McPherson *et al* using a KrF laser at 248 nm, producing pulses of approximately 300 fs with intensities in the region of 10^{15} W cm^{-2} [113]. They observed up to the 17th harmonic in neon, which corresponds to 12 photons above threshold. Using a longer wavelength, 1064 nm. Ferray *et al* reported the observation of harmonics from argon, krypton and xenon. They produced spectra that exhibited what have now been recognized as typical characteristics for harmonic spectra [96]. Such a spectrum is shown in figure 3 and the main observable characteristics are: a rapid decrease in harmonic intensity from third to seventh order; a plateau region that extends out to 27th order, with the harmonics having similar intensities; and a rapid drop in harmonic strength beyond the 27th order. These features have been observed in the spectra of many atoms, although of course the precise details vary [96, 97, 114, 115].

Initially it was unknown whether these characteristics were caused by single atom effects or by propagation effects due to the passage of the radiation through the collection of atoms and ionized electrons in the atomic beam. However many theoretical

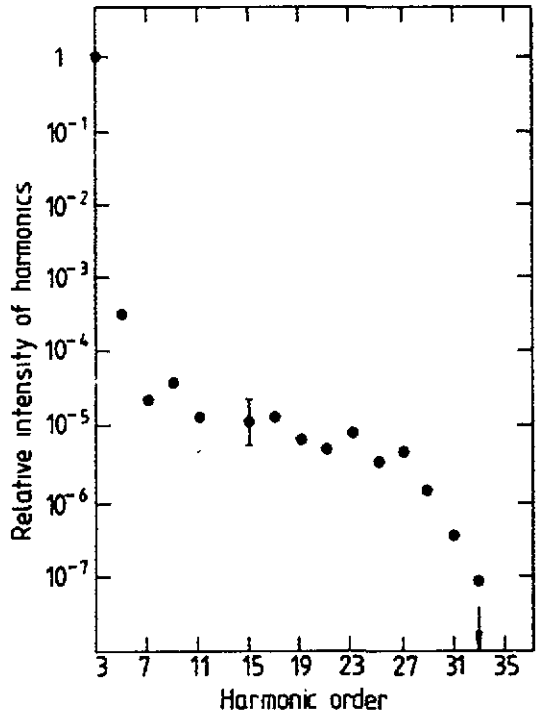

Figure 3. Harmonic spectrum from argon at a laser intensity of approximately 3×10^{13} W cm^{-2} at 1064 nm, from [96].

single atom calculations have reproduced many of these characteristics, suggesting that they are predominantly single atom effects [88, 92, 95, 100, 116–119]. Indeed even a simple system such as two bound states, or one bound state and a continuum in a monochromatic field will reproduce these characteristics, implying that they are generic to a strongly driven non-linear system [119, 120].

Theoretical calculations of both ATI and harmonic spectra have provided indications of the physical basis of these characteristics [116]. The plateau begins to appear when the multiphoton transition required to produce the harmonic occurs from a continuum state and not a bound state. The abrupt cut-off of the plateau at high energy corresponds to where the magnitude of the ATI peaks decreases. In the plateau region, the ATI peaks are of a similar magnitude and so correspondingly are the harmonics [117]. Of course we should remember that the observed signal is a bulk many-atom response. The high frequency radiation could well break the necessary phase matching and terminate the plateau of harmonics.

In this review, we shall limit ourselves to considering an area of great interest at present because of the recent reports of very high order harmonic generation, and only consider the generation of harmonics in electric fields that are close to the critical value for OTB ionization to occur [34].

4.1. High order harmonic generation

Before we begin to discuss any theoretical calculations of harmonic spectra, we must first deal with the exact method by which these spectra are obtained. The usual method

for calculating a power spectrum is to simply take the modulus squared of the Fourier transform of the dipole expectation value (in atomic units),

$$|D(\omega)|^2 \propto \left| \int_0^t \langle \psi(r, t) | \boldsymbol{d}(t) | \psi(r, t) \rangle \, e^{-i\omega t} \, dt \right|^2 \tag{18}$$

where $\boldsymbol{d}(t)$ is the atomic dipole moment. This is relatively straightforward to calculate. However the power, V, radiated by a dipole moment into all directions is given by [119, 121]

$$P = \frac{2e^2}{3c^3} \left\langle \frac{d^2 r}{dt^2} \right\rangle. \tag{19}$$

The difference between taking the expectation value of the dipole moment and the expectation value of the acceleration is normally accounted for by simply multiplying the spectrum of radiated light calculated from equation (18) by ω^4 [119] (although some authors ignore it altogether [92, 95, 116, 117]). Unfortunately this is strictly not correct, because the dipole moment and its velocity do not vanish at large times, particularly when significant amounts of ionization are produced during the laser pulse, when large final dipole moments are produced. Therefore it is more satisfactory to use the acceleration directly using Ehrenfest's theorem (in atomic units):

$$\ddot{\boldsymbol{d}}(t) = \frac{d^2}{dt^2} \langle r \rangle = \left\langle -\frac{\partial H}{\partial r} \right\rangle \tag{20}$$

where H is the interaction part of the Hamiltonian of the system (atomic and laser field interactions). This way of obtaining the acceleration of the atom is extremely useful computationally as it depends mainly on the part of the wavefunction where the electron experiences the greatest force. Any wavefunction far from the core and any asymptotic value of the dipole moment is irrelevant.

It must also be pointed out that calculating the harmonic spectrum by Fourier analysing the expectation value of the time-dependent electronic acceleration is only an approximation. In actual fact a more precise procedure is to use the autocorrelation function of the acceleration. The spectral density of the emitted radiation is then the Fourier transform of this. This has been discussed by many authors [119, 122] and used directly by LaGattuta [123] in the calculation of single atom high harmonic spectra. However it should be remembered that the observed radiation results from many spatially separated atoms. The individual quantum dipoles can be thought of as the sum of a mean atomic dipole and a random fluctuation. The mean dipoles have the phase of the exciting radiation imprinted upon them and in the forward direction they can sum coherently to a cooperative output which varies quadratically with the atomic density. The fluctuation terms have no such phase imprint and sum incoherently as spontaneous near-isotropic noise varying linearly with density.

At low intensities, the dominant method of ionization is multiphoton excitation to real or virtual bound levels and thence out into the continuum. For long pulses, the photoelectron spectrum consists of well defined ATI peaks separated by the photon energy. For short pulses, these ATI peaks split up into several subpeaks, many of which can be accounted for in terms of multiphoton resonances between AC Stark-shifted bound states [118, 124].

Similarly, when the harmonic spectra produced by these pulses are examined, they consist of peaks at odd multiples of the photon energy, again modified by the occurrence

of bound state resonances [92, 97, 125, 126]. If such resonances do occur, then the particular harmonic that corresponds to the order of the multiphoton resonance can be dramatically enhanced: however, such enhancement can only affect a single harmonic. To increase the magnitude of all the harmonics, one can instead increase the incident laser intensity.

Recent experiments have shown that high intensity lasers are capable of producing both high-order and relatively high strength harmonics [17]. However there is a limit to the increase that one can make to the intensity and still generate an observable single atom harmonic spectrum. To examine the effect of intensity on the harmonic spectrum we can roughly divide the ionization process into two regimes. In the first regime, applicable at low intensities, ionization occurs by the electron passing through a series of virtual levels in the atom, (real levels if a resonance exists), and out into the continuum, where it can continue to absorb photons and form the higher ATI peaks. Harmonics are generated by transitions between these bound levels, or from the continuum to these bound levels [127].

In the second regime, ionization occurs by an alternative mechanism. At low intensities, in static fields, we can think of the atomic potential as being distorted by the incident electric field, so that the bound electron 'sees' a potential barrier in the direction of the electric field polarization. However above a certain critical incident electric field, defined by static field theory, the potential barrier is low enough that the electron can pass directly over it (see figure 4). This is a rapid process. For an oscillating electric field, a similar process can occur at optical frequencies provided that the incident electric field is greater than the critical field for some portion of its cycle. In a typical laser pulse, ionization can occur within half of a laser field cycle, once the critical field is reached.

Of course, the division of ionization into these two regimes is arbitrary. The pictures represent two extreme views of the ionization process and for intermediate intensities one can view the ionization process as having some contribution from the electron

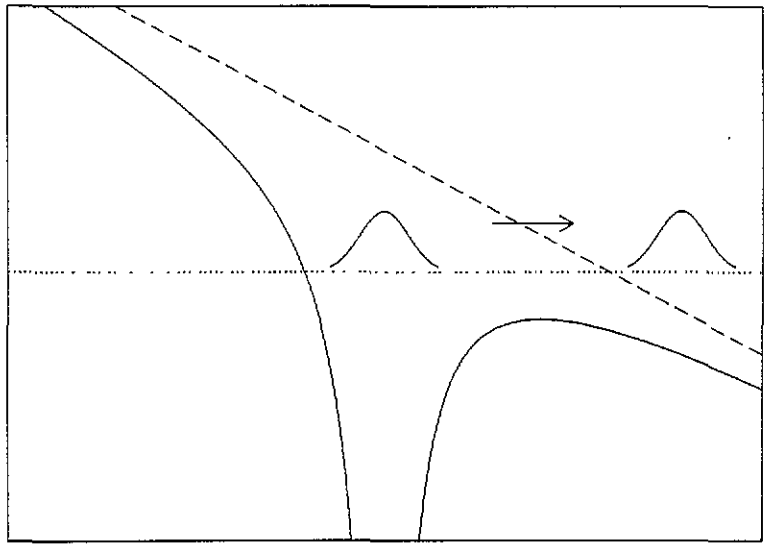

Figure 4. Schematic diagram of over-the-barrier ionization. The broken line represents the incident electric field, the dotted line represents the zero-field bound state energy and the full curve represents the resultant potential of the electric and atomic fields.

tunnelling through the barrier presented by the resultant potential [128], or alternatively ionization can occur when the electron is excited to higher levels and then passes directly over the barrier. However, considering over-the-barrier (OTB) ionization and multiphoton absorption ionization as two distinct processes can be useful, because one can then attempt to interpret the relatively abrupt changes in the photoelectron and harmonic spectra that do occur as the intensity increases.

This picture of over-the-barrier ionization has been used previously with success by Augst *et al* [129]. By using a simple classical time-independent picture of OTB ionization, they have shown that there is good agreement between the intensities at which OTB ionization is predicted and the experimentally measured appearance intensities.

To illustrate how the ionization processes affect the photoelectron and harmonic spectra, we can use the results of a direct numerical integration calculation using a one-dimensional model potential, $V(x) = -1/(1+x^2)^{1/2}$. This type of calculation has been used to produce many of the results in this review. Figures 5 and 6 show harmonic and photoelectron spectra for two intensities: the lower intensity, 2.0×10^{14} W cm^{-2}, is below the critical intensity and the other, 3.2×10^{15} W cm^{-2}, is above. The critical intensity for the model potential is approximately 5×10^{14} W cm^{-2}. All the plots are for an incident pulse of wavelength 300 nm and pulse length of 50 fs. Figures 5(a) and 6(a) show the effect that increasing the peak intensity has on the harmonic spectrum: there has been a slight *decrease* in harmonic generation at the higher intensity and the background has increased by orders of magnitude. Examining the photoelectron spectra for these two intensities (figures 5(b) and 6(b)), one can see that the ATI peaks cease to be distinguishable at the higher intensity, showing a close correlation between the photoelectron and harmonic spectra.

One can explain the slight decrease in harmonic strength at higher intensities in terms of the ionization mechanism. When an atom ionizes by multiphoton absorption, the ionizing electron passes through a series of virtual bound levels of the atom (some of these levels may be real if any multiphoton resonances occur). This process is *periodic* and relatively *slow*, because the matrix element of the multiphoton transition is small. Also the electron remains close to the nucleus and so it can absorb further photons, or alternatively emit harmonics. In addition, when the electron is promoted into the continuum, it is *still close to the nucleus* and hence capable of emitting high-order harmonics.

In contrast, ionization by the OTB mechanism is a very rapid process once the critical electric field is reached, as can be seen from figure 6. Once over the potential barrier, the electron accelerates down the potential and away from the nucleus. It is the *rapidity* and *aperiodic* nature of this process that prevents further harmonic generation. The wavepacket *quickly moves away from the core* and there is very little time for harmonics to be generated.

The response of the electron to the incident electric field during the remaining part of the pulse becomes that of a free electron and the electron can scatter from the nucleus as it moves away. Such scattering events modify the harmonic spectrum by increasing the background. This is significant experimentally because this background can be large enough to wash out any harmonics produced on the rising edge of the pulse before the critical field is reached, because the contrast between the peaks and the background is small. This background grows dramatically with increasing peak intensity. It is this scattering background that destroys any regular structure in the photoelectron spectrum.

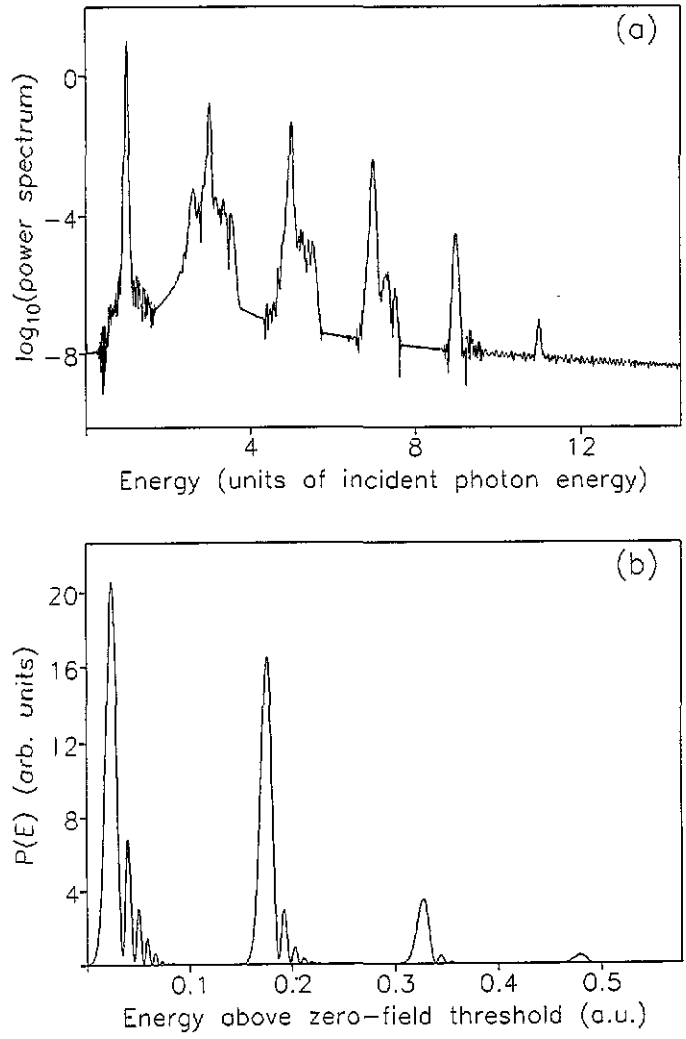

Figure 5. Figures showing the computed (*a*) harmonic spectrum and (*b*) photoelectron spectrum from a 50 fs (50 cycles) pulse of wavelength 300 nm and peak intensity 2×10^{14} W cm^{-2}.

It is interesting to notice that the peaks at the higher intensity are only one order of magnitude greater than the background. Thus such intense pulses could possibly be used to create a flash of high energy, broad band radiation in a time comparable to the incident laser pulse. This could be an important source of soft x-ray radiation.

It is interesting to compare these observations with those obtained by considering classical atoms. Chu and Yin [130] have used the technique developed by Leopold and Percival [131] to examine classical atoms exposed to electric fields greater than the critical field at optical frequencies. Amongst other mechanisms, they identify a direct ionization mechanism that can be considered to be the classical analogue of over-the-barrier ionization. Once initiated, such ionization proceeds within a fraction of a cycle, as is noticed in our quantum mechanical calculation. Bandarage, Maquet and Cooper have also identified this direct ionization process [132]. Furthermore, they

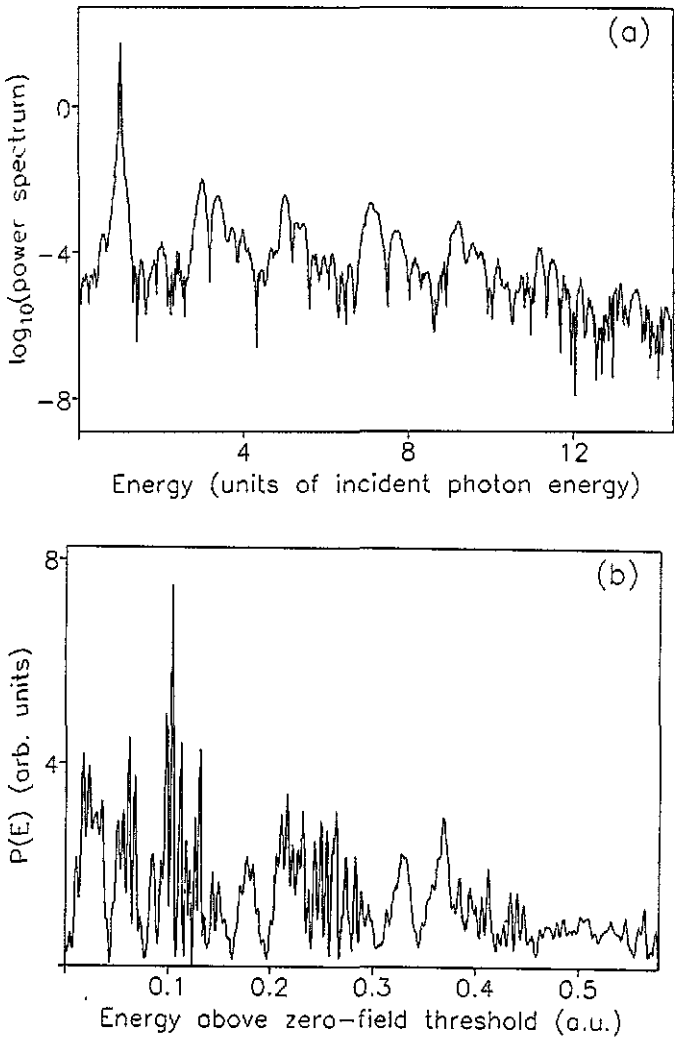

Figure 6. Same as figure 5 but with a peak intensity of 3.2×10^{15} W cm^{-2}.

have reported that once ionized, the electron in the laser field generates a background to the harmonic spectrum, which is consistent with the quantum mechanical results.

4.2. Phase matching effects

Harmonic generation occurs because the induced dipole of an atom has prominent frequency components at multiples of the driving frequency. In a single atom calculation, only the response of an individual atom is calculated, but experimentally this radiation is affected by its passage through the medium, i.e. a gas jet. There is considerable interest at present in the effect of the propagation through the medium on the single atom spectrum: for long pulses (>1 ps) the theoretical models agree so well with the experimental spectra, that propagation effects appear to be unexpectedly small [95, 133].

propagate through a medium at different speeds and therefore become out of phase with the driving field. Thus the harmonics produced by each individual atom have a different phase and these produce a decrease in the total harmonic strength measured. Furthermore, the focusing of the pulse introduces a geometric phase slip across the focus that is different for each harmonic. These mismatches increase dramatically with increasing harmonic order.

Recent experimental work by the Saclay group has established the relative importance of these phenomena [133].

5. Suppression of ionization

The majority of multiphoton ionization experiments are carried out on multielectron atoms, for example, neon, xenon or helium. If an ultra-intense laser field irradiates such an atom, then the ionization rate can be significant and even with picosecond pulses, all the atoms can be ionized well before the peak of the pulse. The ions formed can also have rapid ionization rates and it will only be highly ionized species that are actually exposed to the peak of the pulse [134]. However if some mechanism exists by which ionization is suppressed, then it may be possible to expose neutral atoms to high intensity laser fields. Various mechanisms have been suggested that could bring about ionization suppression. We can broadly divide these into two types. The first type we term as quantum interference suppression, because the mechanisms of this type are generally interpreted in terms of destructive interference between the ionization from closely spaced bound states. The second general type is a subject of great topical interest at present and can be labelled as super-intense field ionization suppression: such suppression typically occurs in fields of $10^{17}\,\mathrm{W\,cm^{-2}}$ or greater and has to do with the production of electronic wavepackets which oscillate in the laser field with large amplitudes far from the nucleus with diminished ability to absorb photons.

So far little experimental work has been performed to study ionization suppression. Particularly for super-intense field ionization suppression, the experimental laser parameters that must be achieved lie beyond the capabilities of today's technology: we will discuss these parameters below. However, experiments have been performed to examine what we have labelled as quantum interference suppression. We will return to these experiments below.

5.1. Quantum interference ionization suppression

Two similar processes have been suggested that would bring about ionization suppression by the quantum interference of the ionization amplitudes from a coherent wavepacket of states close to the initial state [56, 135]. Cardimona *et al* have pointed out that quantum interference can be thought of in terms of dipole moments [136]. In a simple example, if an atom consists of two upper states and a lower state, then an incident laser field will generate a coherent oscillating dipole moment for each transition. The phase relation between the two dipoles will depend on the laser detuning. There will be a particular detuning at which the two dipoles will have a phase difference of π and equal amplitudes. If the polarizations of the dipoles are the same, then the total dipole moment will vanish and the atom will be decoupled from the field, hence there will be no fluorescence. Cardimona *et al* extend this picture to the case of multiphoton ionization: the condition for zero population transfer into the continuum is simply that the net Rabi frequency from the bound states to the continuum states is zero.

One of the above-mentioned population trapping mechanisms was studied by Parker and Stroud, through a series of numerical models [135]. They have shown that if there are other bound states of the same parity as the initial state separated from the initial state by less than the bandwidth of the laser, then the ionization from these states can interfere and reduce the ionization rate to less than that predicted by Fermi's golden rule. Population moves out of the initial states and into the other states by Raman coupling transitions through the continuum [137]. Thus the field produces not just ionization, but also stimulated recombination. It is this recombination that results in the coherent superposition of the bound states, which inhibits further ionization. Parker and Stroud identify this effect using a simple model of three bound states, equally spaced in energy and with the same parity and angular momentum quantum number. The continuum is modelled by a quasicontinuum of equally spaced levels, each level having the same dipole moment coupling to the bound states, and an angular momentum quantum number one greater than the bound states. Population trapping is identified for a large variety of pulse shapes, dipole moments and energy level spacings. The parameters used for this study were chosen so that Fermi's golden rule predicted that 90% of the population would be ionized in the pulse, so a pulse of intensity 2×10^{14} W cm^{-2}, wavelength 364 nm and a full width half maximum of three optical cycles was used. The population was initially in the $l=2$, $n=3$ state.

We must point out that the wavepackets formed by the above process are different from the so-called depletion wavepackets studied by Zoller and others [138]. Here we are concerned with what can be termed as Fourier wavepackets which are formed by short pulses. The pulse lengths are less than the classical orbit time for the Rydberg states being accessed and the wavepacket is formed by the short pulse promoting some small part of the ground state population directly into the Rydberg states. The evolution of the wavepacket then occurs in zero field. Depletion wavepackets, however, are formed by long laser pulses and the pulse lengths used are longer than the classical orbit time of the Rydberg states accessed. During the pulse, the ground state is completely depleted and the wavepacket formed, which moves away from the nucleus, until it is radially localized at too great a distance to interact with the laser field further. Whilst the pulse is still present, the wavepacket then travels back towards the nucleus and again interacts with the laser field, and population then transfers either back into the ground state or out into the continuum. For long enough pulses, this can happen several times.

Fedorov and Movsesian have identified a mechanism that leads to the stabilization of a Rydberg atom [56]. States adjacent to the initial Rydberg-state are coherently populated by Raman coupling transitions via the continuum and other bound states. It is the transitions from this group of Rydberg states to the continuum that interfere with each other and cancel so as to inhibit the ionization. There is very little similarity between the Rydberg wavepacket produced by this Raman coupling mechanism and a 'classical' Rydberg wavepacket [139, 140]. A 'classical' wavepacket is produced by an ultrashort pulse and consists of a cluster of closely-spaced energy levels. The intent is to produce a wavepacket with a motion that closely approximates a classical Kepler orbit. By contrast, the wavepacket produced by purely quantum mechanical interference effects is not localized in space. This is in contrast with the 'classical' Rydberg wavepacket, where the number of states involved can be large and the wavepacket is localized. Fedorov and Movsesian suggest that microwave ionization may be used to examine this population trapping mechanism experimentally. Possible experimental parameters for the observation of this type of ionization suppression would be $\lambda=$

300 μm, at intensities of the order of 10^5 W cm^{-2}, in a microwave cavity about 0.1 m in length [56].

Finally, quantum interference plays a part in interpreting what occurs when a Rydberg wavepacket is formed by the *indirect* population of a number of highly excited energy levels. When a Rydberg wavepacket is created by *direct* excitation, a compact wavepacket is formed, centred on the nucleus, which easily ionizes in a high intensity laser field. In this case, the laser is tuned to a highly excited level and because of the close spacing of the adjacent levels, several levels are populated by the finite bandwidth of the laser. If instead the laser is tuned close to a lower excited level, e.g. the $n = 5$ level, then the bandwidth of the laser is not sufficient to directly excite the adjacent levels, but instead other levels can only be accessed by a two-photon Raman coupling process through the continuum and other bound levels of the atom. As the pulse progresses, the higher Rydberg levels become populated by repeated Raman coupling transitions and the population from the $n = 5$ state moves into the higher states. This has been studied by Burnett *et al* [141] and Piraux *et al* [58].

The population from the initial state does not move into the high-lying Rydberg states directly, but rather through a three-photon process: from the initial state into the $n = 5$ state and then through a two-photon Raman process into the Rydberg state. So the wavepacket formed from the higher Rydberg levels is driven away from the nucleus. Of course, when the electron is not localized near the nucleus it is quasifree and cannot absorb further photons to ionize, so the interaction of the spatially extended wavepacket with the field is weak and the ionization is inhibited.

As more higher-lying Rydberg states are accessed the wavepacket becomes localized further from the nucleus. It is this spreading that prevents the overlap of the wavepacket with the nucleus being large at any time, because most of the wavepacket is localized far enough away from the nucleus so that even the oscillation of the wavepacket in the external laser field (of the order of one atomic unit) does not bring it close enough to the nucleus to result in a substantial ionization.

Recently, important experiments have been performed to study this type of ionization suppression. These are the first to report the observation of stabilization and the mechanism used to interpret the results is that of Burnett *et al*, involving the formation of a wavepacket of bound states that is localized some distance from the nucleus and hence with a low ionization rate. Jones and Bucksbaum performed such an experiment using barium exposed to a laser of intensity 10^{14} W cm^{-2} [142]. It was found that the single photon ionization of the outer electron in a barium 6snk Stark-state can be suppressed relative to the three-photon ionization of a tightly bound 6s core electron. They identify the formation of an extended wavepacket by Raman coupling as the suppression mechanism, following the work of Burnett *et al* described above [141]. A recent experiment by Noordam *et al* [143] observed the redistribution of population amongst Rydberg levels by Raman coupling, and the results were also interpreted in the same terms.

5.2. Super-intense field ionization suppression

In contrast to the ionization suppression processes outlined above which typically occur at intensities below 10^{15} W cm^{-2}, a second suppression mechanism involves super-intense fields. In such intense fields, instead of the atom ionizing swiftly by over-the-barrier ionization, it appears that at suitably high frequencies, the ionization rate can be severely reduced so that it is negligible on the time scale of a laser pulse. In the 1970s, several researchers including Mittleman, Gavrila and others began to

realize that atoms in super-intense high-frequency fields can become stabilized with increasing intensity; Gavrila and co-workers then made an extensive analytical and numerical study of the properties of adiabatic states at constant intense field amplitudes and their ability to withstand ionization [144]. The first prediction of stabilization in a pulsed field was made by Su *et al* using their 1D potential model [82]. Pont *et al* [144] initially performed calculations for atoms in the limit of an infinitely high frequency laser field, and concluded that in such fields, the atom is stable to ionization. This was a dramatic conclusion, but of course the infinite frequency is physically unrealistic. However, further calculations indicated that provided the incident frequency is high enough, the ionization rate from an atom in a super-intense field will actually *decrease* with increasing intensity, once some critical intensity is passed (see figure 7) [145].

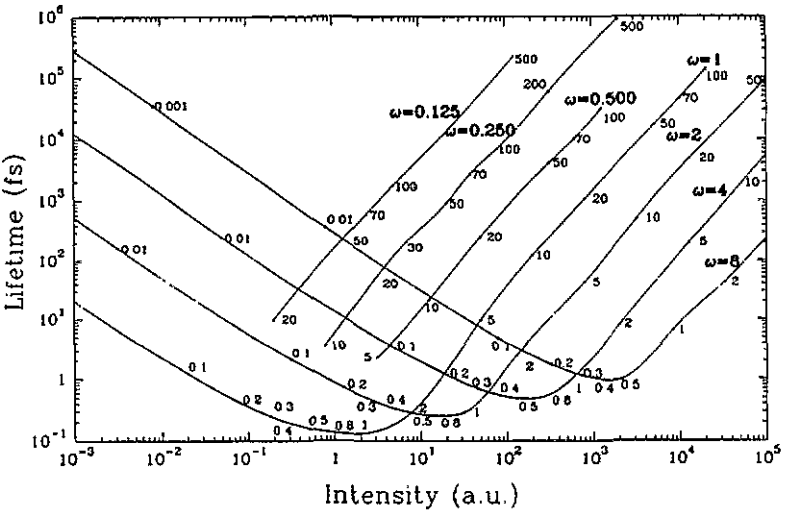

Figure 7. Plot of lifetime atom against intensity for various values of angular frequency. The numbers adjacent to the points give the corresponding values of α_0 [145].

These calculations [144, 145] and subsequently those of other workers [146–149] were carried out in the Kramers–Henneberger frame. This frame has also proved invaluable in interpreting the suppression mechanism as we will demonstrate below. The Kramers–Henneberger (KH) [150, 151] frame is the frame of motion of a free electron in the incident laser field. In this frame the effect of the time-dependent incident electric field is transformed to the time dependence of the atomic potential. Hence the minimal coupling Schrödinger equation

$$i\hbar\frac{\partial\psi}{\partial t}(r,t)=-\frac{\hbar^2}{2m}\nabla^2\psi(r,t)-\frac{i\hbar e}{m}A\cdot\nabla\psi(r,t)+\frac{e^2}{2m}A^2\psi(r,t)+V(r)\psi(r,t) \tag{21}$$

is then transformed to

$$i\hbar\frac{\partial\psi_{KH}}{\partial t}(r,t)=-\frac{\hbar^2}{2m}\nabla^2\psi_{KH}(r,t)+V(r+\alpha(t))\psi_{KH}(r,t) \tag{22}$$

under the KH transformation. The transformation is explicitly given by

$$\exp\left[\frac{ie^2}{2m\hbar}\int_{-\infty}^{t}A^2(\tau)\,d\tau\right]\exp\left[-\frac{e}{m}\left(\int_{-\infty}^{t}A(\tau)\,d\tau\right)\cdot\nabla\right] \tag{23}$$

where

$$\boldsymbol{\alpha}(t) = -\frac{e}{m}\int_0^t \boldsymbol{A}(t')\,\mathrm{d}t'. \tag{24}$$

This is the displacement of a free electron in the incident laser field. For steady field conditions, i.e. $\boldsymbol{\mathcal{E}}(t) = \boldsymbol{\mathcal{E}}_0 \sin\omega t$, and we can write $\boldsymbol{\alpha}(t) = \boldsymbol{\alpha}_0 \sin\omega t$; ($\boldsymbol{\alpha}_0 = e\boldsymbol{\mathcal{E}}_0/m\omega^2$, which equals the amplitude of oscillation of a free electron in the field). To illustrate how the KH frame is useful in interpreting super-intense field ionization, let us follow the work of Gavrila *et al* [152], and consider a pulse where the electric field amplitude is steady. Under these conditions, we can write our KH frame wavefunction in atomic units in Floquet form:

$$\psi(\boldsymbol{r}, t) = \mathrm{e}^{-\mathrm{i}E_{\mathrm{KH}}t}\sum_{n=\infty}^{\infty}\psi_n^{E_{\mathrm{KH}}}(\boldsymbol{r})\,\mathrm{e}^{-\mathrm{i}n\omega t} \tag{25}$$

where E_{KH} is the Floquet quasi-energy. (From now on we will adopt the convention of atomic units.) The KH frame potential can be Fourier decomposed thus

$$V(\boldsymbol{r}+\boldsymbol{\alpha}(t)) = \sum_{m=-\infty}^{\infty} V_m(\boldsymbol{\alpha}_0; \boldsymbol{r})\,\mathrm{e}^{-\mathrm{i}m\omega r} \tag{26}$$

where the coefficients can be written in the form

$$V_m(\boldsymbol{\alpha}_0; \boldsymbol{r}) = \frac{\mathrm{i}^m}{\pi}\int_{-1}^{+1} V(\boldsymbol{r}+\boldsymbol{\alpha}_0 u)\,T_m(u)(1-u^2)^{-1/2}\,\mathrm{d}u \tag{27}$$

where $T_n(u)$ are Chebyshev polynomials.

Inserting equations (25) and (26) into the KH frame Schrödinger equation (equation (22)) yields a set of coupled differential equations for the components of $\psi(\boldsymbol{r})$:

$$\left(-\tfrac{1}{2}\nabla^2 + V_0(\boldsymbol{\alpha}_0; \boldsymbol{r}) - (E_{\mathrm{KH}} + n\omega)\right)\psi_n^{E_{\mathrm{KH}}}(\boldsymbol{r}) = -\sum_{m=-\infty}^{\infty} V_{n-m}\psi_m^{E_{\mathrm{KH}}}(\boldsymbol{r})_{(m\neq n)}. \tag{28}$$

If the coupling terms on the right-hand side could be neglected, then we could replace the time-dependent KH frame potential $V(\boldsymbol{r}+\boldsymbol{\alpha}(t))$ by $V_0(\boldsymbol{\alpha}_0; \boldsymbol{r})$, which is simply the time-averaged KH frame potential. The Schrödinger equation would then be written as

$$-\tfrac{1}{2}\nabla^2\psi_0(\boldsymbol{r}, t) + V_0(\boldsymbol{\alpha}_0; \boldsymbol{r})\psi_0(\boldsymbol{r}, t) = E_{\mathrm{KH}}\psi_0(\boldsymbol{r}, t). \tag{29}$$

This is now a *time-independent* Schrödinger equation and we can describe our system in terms of a set of eigenstates of the atom and laser field. There are no transitions between these eigenstates and hence our atom is *stable to ionization.*

Gavrila and Kaminski [152] pointed out that the condition for which the V_n ($n \neq 0$) are zero is that the incident laser frequency is infinitely large. More importantly, Pont and Gavrila [145] showed that when the conditions

$$\omega \gg |E_{\mathrm{KH}}| \tag{30}$$

and

$$\alpha_0^2\omega \gg 1 \tag{31}$$

are fulfilled, where E_{KH} is the binding energy of the binding energy of the KH frame eigenstate, then we can consider equation (29) as a good lowest order approximation to our system. These are the conditions stated above that the frequency and intensity of the applied laser field are both large. The V_n ($n \neq 0$) can then be considered as perturbations to the lowest order eigenstates of equation 29 and hence one can find the effective ionization rates from these states. Pont and Gavrila [145] carried out such

calculations and produced a plot of the lifetime of the ground state against intensity for various angular frequencies (figure 7). The graph showed distinct minima in the lifetimes at critical intensities that varied with the angular frequency. Beyond these critical intensities, the lifetime of the state *increased* with increasing intensity: we can consider that the ionization from the atom is suppressed.

As one might expect the atom is severely distorted by these super-intense laser fields. If we can describe our atom as comprising one or more eigenstates of the lowest order KH frame potential, then studying the shape of these states can be instructive. The $V_0(\boldsymbol{\alpha}_0; \boldsymbol{r})$ potential for $\alpha_0 > 1$ has a distinctive dichotomous (two-peaked) shape, with the two lobes being separated by an distance approximately equal to $2\alpha_0$. Hence the lowest energy eigenstates are dichotomous (see figure 8, which shows the KH eigenstates for our one-dimensional calculations), with the $n = 1, 2$ states being degenerate at large α_0 [144, 146, 153–155]. For smaller α_0 ($\alpha < 1$), this splitting is only partial, but for large α_0 ($\alpha_0 > 1$) the potential is extremely shallow at the centre and the dichotomous splitting is almost complete. The time-averaged potential is considerably shallower than the zero-field potential and this represents a decrease in the binding energy in super-intense fields (in contrast to the case in lower intensity fields). Pont *et al* report that for a hydrogen atom, the binding energy of the ground state is reduced by a factor of $\alpha_0^{2/3}$ as compared to the ground state energy. In figure 8 we show the shapes of the lowest few KH bound eigenstates for laser parameters that result in a value for α_0 of 18.49. For this value, the lowest two states are in effect degenerate and the wavefunction is highly dichotomous. The $n_{KH} = 3$ state is the lowest state with significant probability at the nucleus.

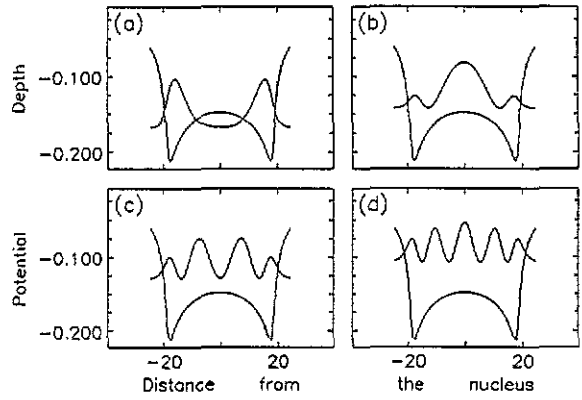

Figure 8. Modulus-squared of the KH bound eigenfunctions for $\alpha_0 = 18.49$. In (*a*) the $n_{KH} = 1$ eigenfunction is plotted (the modulus-squared of $n_{KH} = 2$ is almost identical). In (*b*)–(*d*), the $n_{KH} = 3,4$ and 5 eigenstates respectively are shown.

However as Pont and Gavrila pointed out, an atom does not suddenly appear in a super-intense laser field, but instead it is exposed to sub-critical fields during the ramp of the pulse. By examining Pont and Gavrila's plot of lifetime against intensity, (figure 7), we can see that if an atom in a ground state is exposed to a ramped pulse, then it must pass through what has become known as a 'death valley', where it is exposed to an intensity where the lifetime of the atom is a minimum and is too short to survive the pulse without being ionized.

However, Pont and Gavrila only discussed the adiabatic case where a single atomic state is occupied. More realistically, we can consider an atom that is exposed to a

time-dependent laser pulse, with the atom no longer being restricted to only the ground state of the time-averaged KH frame potential. To examine what effect a pulse turn-on has on the KH frame eigenstate populations, various calculations have been performed [78, 84, 89, 146, 147, 156]. The calculations have varied substantially in their different approaches; some are straightforward numerical integrations of the Schrödinger equation in one or three dimensions [78, 89, 147, 156], some use the Kramers-Henneberger frame directly [144–146, 153, 155] and others use classical techniques [109, 157].

The particular calculation that has been carried out to produce the remaining figures in this article consists of a Crank–Nicholson time integration routine that solves the one-dimensional time-dependent Schrödinger equation for an atom in a laser field. We have used the model potential $V(x) = 1/(1+x^2)^{1/2}$, which has a Rydberg series of bound eigenstates. Details of the method of calculation can be found in [33]. We are justified in using the non-relativistic Schrödinger equation for these super-intense laser fields because the frequencies used are so large. This means that the velocity of the electron's oscillatory motion is still small compared with the speed of light. We refer the reader to the review of multiphoton ionization by Mainfray and Manus for a discussion of laser–atom physics in the relativistic regime [158].

In figures 9(*a*)–(*b*), we show the ionization probability as a function of time for two different pulse turn-ons (*a*), the pulse turn-on is 0.25 cycles: this extremely short pulse, as well as being experimentally unrealistic, has such a large bandwidth that most of the population is promoted directly into the continuum and there is no bound population left to be stabilized in the super-intense field. In (*b*) the turn-on time is 5.25 cycles: this is an ideal length because the bandwidth does not give too large an overlap with the continuum, but the atom passes rapidly enough through the lower intensity fields so that not too much of it is ionized. A delicate balance must be struck between turning on the pulse too quickly or too slowly: too quickly and the large bandwidth of the pulse means that a large proportion of the population is promoted straight into the continuum; too slowly and the atom will be ionized before the lifetime of the atom begins to increase. It can be concluded from the work of several authors that up to approximately 80% of the population of the atom can be expected to survive the turn-on of a relatively swift, but smooth, pulse.

Let us now examine in greater detail the ionization of an atom exposed to a pulse with a fast (5.25 cycle) ramped turn-on to illustrate what determines the percentage survival. In figure 10(*a*)–(*c*) we see graphs of the ionisation as a function of time for different laser parameters. In figure 10(*a*) the laser field is large enough to allow for rapid ionization by the wavepacket passing directly over the resultant potential barrier of incident laser field and atomic potentials. Therefore the ionization of the atom is fast and the atom is certainly not stabilized. In figure 10(*b*), the incident laser intensity and frequency are high enough to cause ionization suppression and we can see that the ionization rate is significantly less than that in figure 10(*a*). Finally in figure 10(*c*), we see an extreme case of ionization suppression. The very high frequency and intensity cause the atom to be effectively stabilized in the field: there is no detectable ionization rate on the time scale of the pulse, once initial transients die out.

Let us consider an atom exposed to a pulse of the same parameters as used to produce figure 10(*c*). The fast turn-on prevents all the atomic population moving adiabatically from the ground state of the atom in zero laser field into the lowest bound KH state. Instead the large bandwidth spreads population across all the KH bound states and promotes some directly into the continuum. Precisely how much population

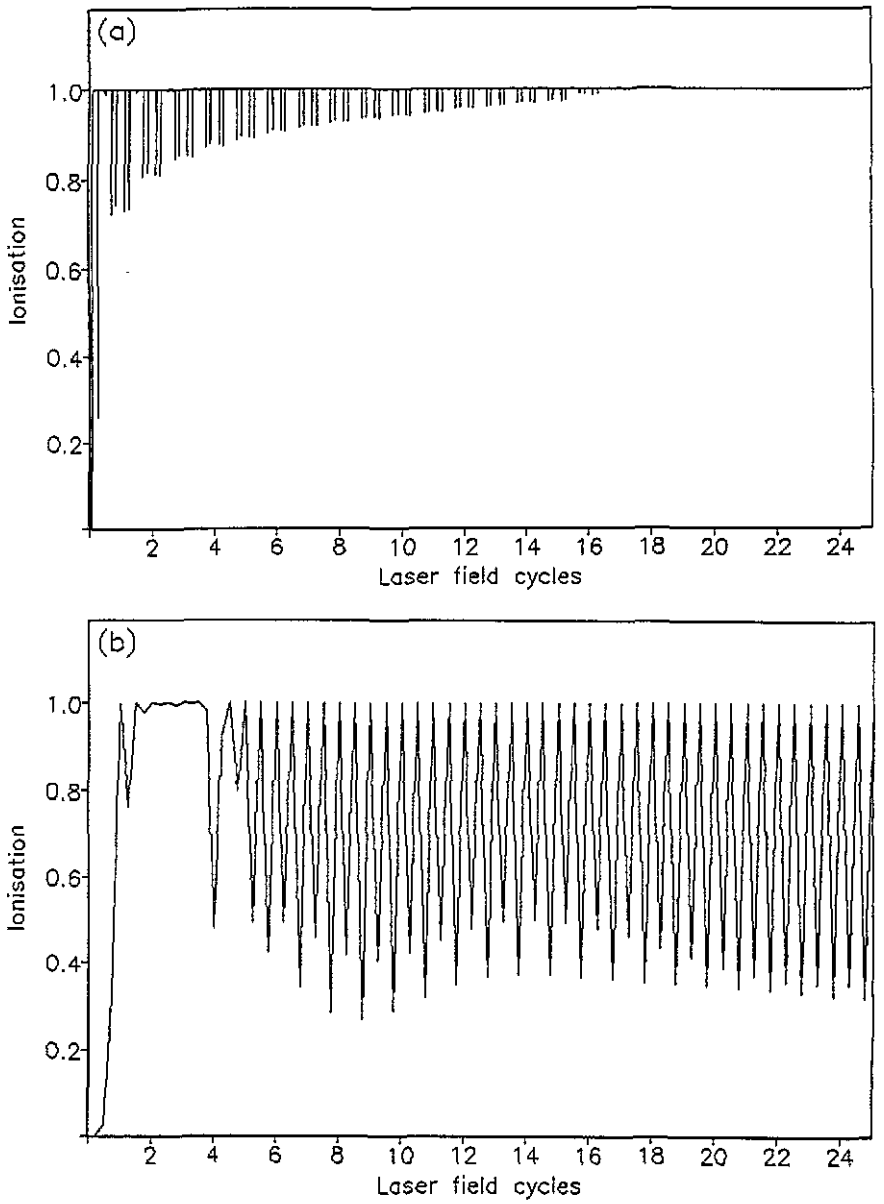

Figure 9. Computed ionization probability as a function of time for a ramped pulse with wavelength 22.8 nm and peak intensity 1.9×10^{20} W cm^{-2}, for (*a*) a 0.25 cycle and (*b*) a 5.25 cycle turn-on.

goes into each individual KH bound state depends very much on the relative overlap of the evolving wavefunction with the KH eigenstates. After the fast turn-on of 5.25 cycles of a high frequency laser field, the atomic wavepacket is still compact, very little changed from its initial form. The KH bound states, however, have a very extended shape, with the ground and first excited states having only a very small overlap with this compact wavepacket. We therefore find that the population moves predominantly into the $n_{KH}=3$ and 5 states, with a small amount of population in the other states.

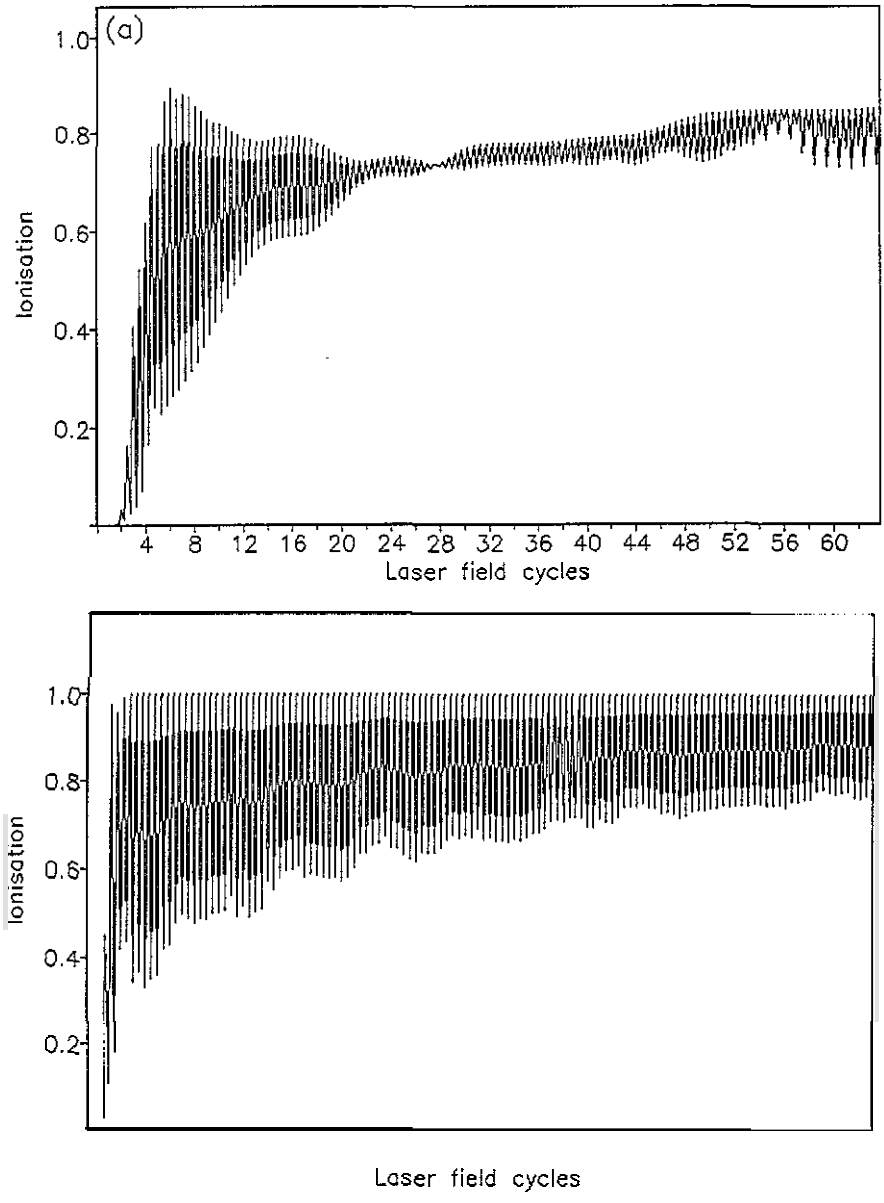

Figure 10. Computed ionization probability as a function of time for ramped pulses with a 5.25 cycle turn-on and various intensities and angular frequencies. The wavelength used is 87.6 nm and the peak intensities are (*a*) 8.78×10^{15} W cm^{-2}, (*b*) 1.40×10^{17} W cm^{-2} and in (*c*), the wavelength is 22.8 nm and the intensity is 1.9×10^{20} W cm^{-2}.

Ignoring the contribution from the continuum states, we can then see that the wavepacket of bound states which make up the wavepacket beat together and the various states move in and out of phase. Furthermore, for finite ratios of $\omega/|E_{KH}|$, there are transitions between the bound states separated by less than the laser bandwidth. In figure 11 we can see the variations of the populations of the KH bound states as the pulse progresses. We can see that the KH populations vary slowly on the timescale of the laser frequency and that population moves into the states initially unpopulated.

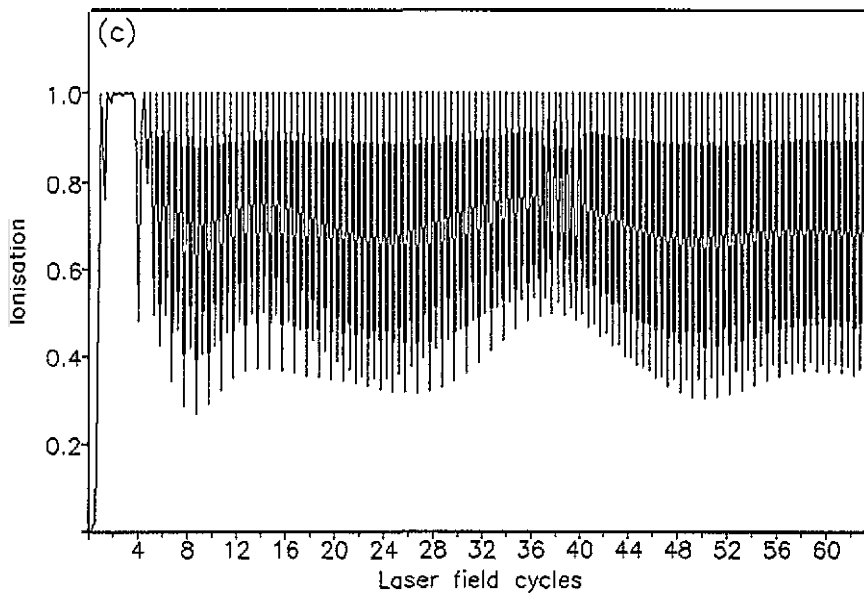

Figure 10. (continued)

In figure 12 the wavepacket of KH eigenstates is shown at different times in the pulse. One can see the $2\alpha_0$ size of the wavepacket, although of course as the various states beat together there can be times when the wavepacket is less than this: this beating goes some way to explain the apparent problem of whether the wavepacket size is α_0 or $2\alpha_0$ which has been discussed previously in the literature.

Of course a 5.25 cycle turn-on is still unrealistically short, but we can however conclude that provided the ramp of any pulse is fast enough so that the atom is only briefly exposed to subcritical fields, ionization suppression may be experimentally observable. To illustrate how little ionization can occur in more realistically smooth pulses, let us examine the predictions of a one-dimensional calculation of the effect on a hydrogenic atom of a smooth pulse of wavelength 22.8 nm, intensity 1.9×10^{20} W cm^{-2} and duration 7.6 fs (figure 13) [155]. At the end of the pulse only approximately 20% of the atom is ionized. (Three-dimensional calculations have been performed by various workers, e.g. [89, 147], and produce results that are similar to the one-dimensional ones.) For this smooth pulse, we still observe a low ionization rate and one can see that the population is still concentrated in the same states that were populated in the pulse turn-on when the distribution of the bound state populations at the end of the pulse is examined (figure 14).

The majority of the calculations that have been performed are concerned with the stabilization of an atom starting in the ground state. The calculations indicate that a high density and high frequency laser field is required for stabilization. By examining the expansion of the KH frame potential $V(\boldsymbol{r}+\boldsymbol{\alpha}(t))$ one can appreciate where the high intensity and frequency conditions arise. The time-dependent potential can be Fourier decomposed as follows

$$V(\boldsymbol{r}+\boldsymbol{\alpha}(t))=\frac{1}{(2\pi)^3}\int \mathrm{d}^3\boldsymbol{k}\,\mathrm{e}^{\mathrm{i}\boldsymbol{k}\cdot\boldsymbol{r}}V(\boldsymbol{k})J_0(\boldsymbol{k}\cdot\boldsymbol{\alpha}) + \sum_{n=1}^{\infty}\frac{1}{(2\pi)^3}\int \mathrm{d}^3\boldsymbol{k}\,\mathrm{e}^{\mathrm{i}\boldsymbol{k}\cdot\boldsymbol{r}}V(\boldsymbol{k})J_n(\boldsymbol{k}\cdot\boldsymbol{\alpha})[\mathrm{e}^{\mathrm{i}n\omega t}+(-1)^n\,\mathrm{e}^{-\mathrm{i}n\omega t}]. \tag{32}$$

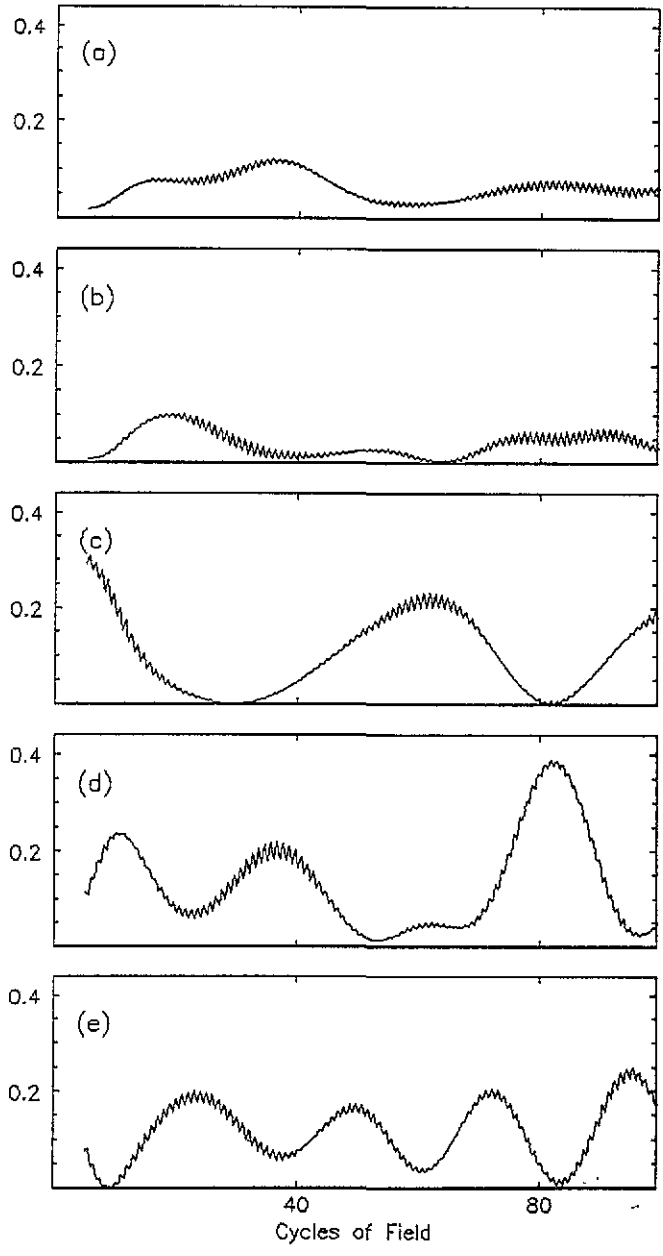

Figure 11. Computed population of the KH bound states as a function of time in a 5.25 cycle ramped pulse of wavelength 22.8 nm and peak intensity 1.9×10^{20} W cm^{-2}. The populations of the $n_{KH}=1$–5 states are shown in (*a*)–(*e*) respectively.

Here the lowest order term corresponds to the time-averaged potential, where $\boldsymbol{k}$ is the momentum vector and $V(\boldsymbol{k})$ is the atomic potential in momentum space. Hence the magnitude of the interaction terms in the KH frame Schrödinger equation are determined by the value of $\boldsymbol{k}\cdot\boldsymbol{\alpha}$. If it is large, then the Bessel functions will be small: $J_0(\boldsymbol{k}\cdot\boldsymbol{\alpha})$ being small implies that the system is weakly bound; the J_n $(n\neq0)$ being small implies that the perturbations to the system are small and the ionization rate is low, For

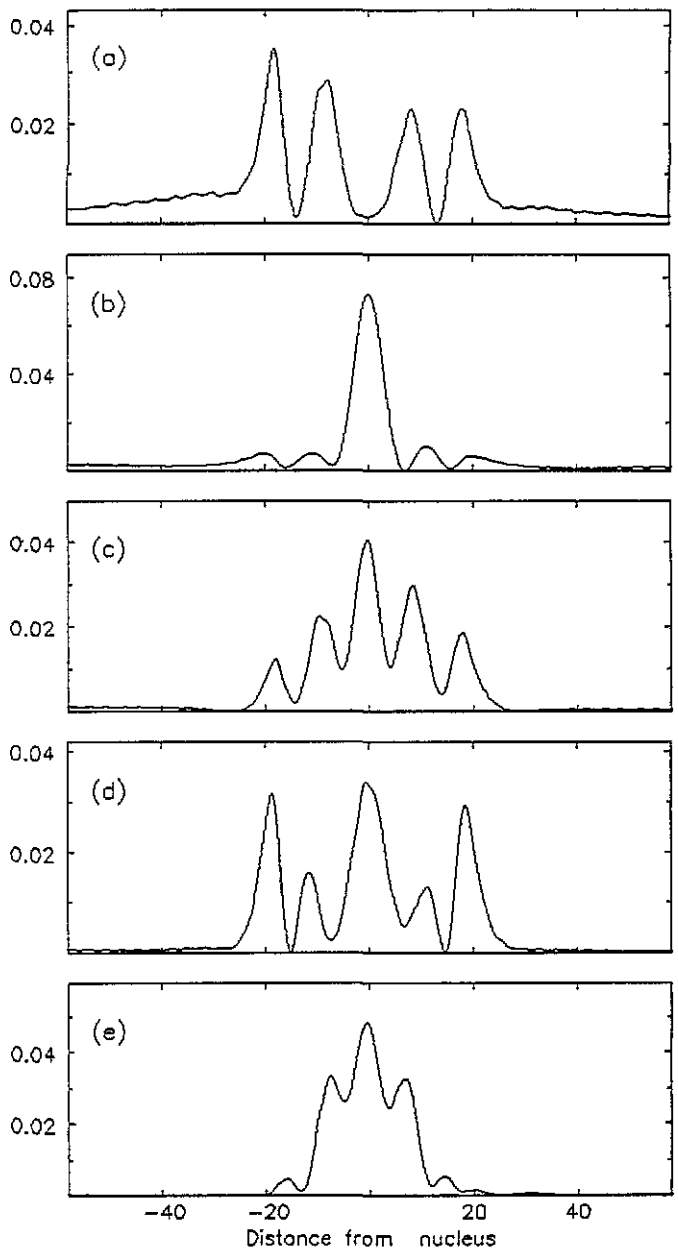

Figure 12. Modulus squared of the wavefunction for the same pulse as figure 11 after (*a*) 30, (*b*) 50, (*c*) 76, (*d*) 96 and (*e*) 158 cycles of the laser field.

electrons being ionized along the direction of the incident electric field, $\boldsymbol{k}\cdot\boldsymbol{\alpha}$ has a value of $k\alpha$ and so the ionization suppression is at a maximum. Moving away from the direction of the electric field, $\boldsymbol{k}\cdot\boldsymbol{\alpha}$ becomes smaller and hence the degree of ionization suppression becomes less. This is in contrast to what occurs at lower (non-suppressing) intensities, where the electrons are preferentially ejected in the direction of the electric field polarization.

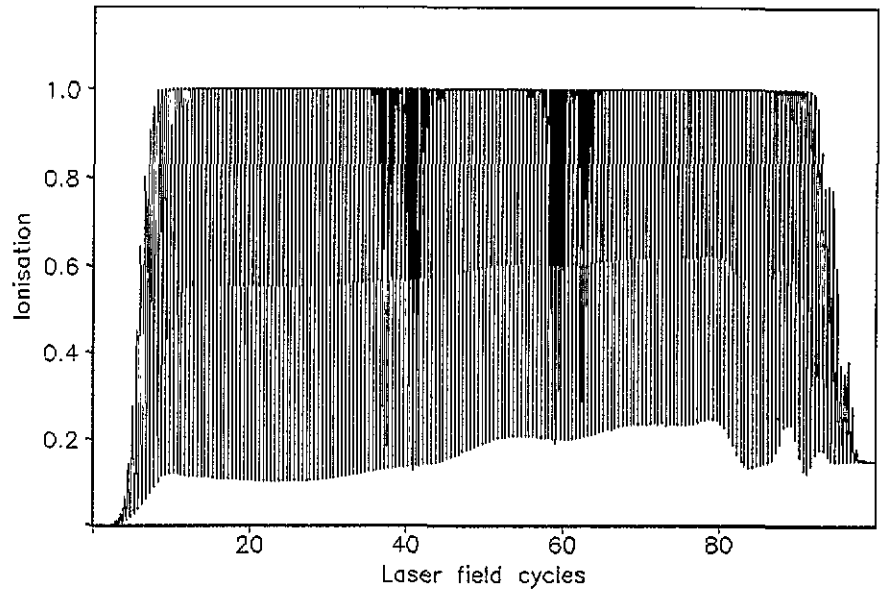

Figure 13. Ionisation probability as a function of time for a 100 cycle smooth sine-squared pulse, with wavelength 22.8 nm and intensity 1.9×10^{20} W cm^{-2}.

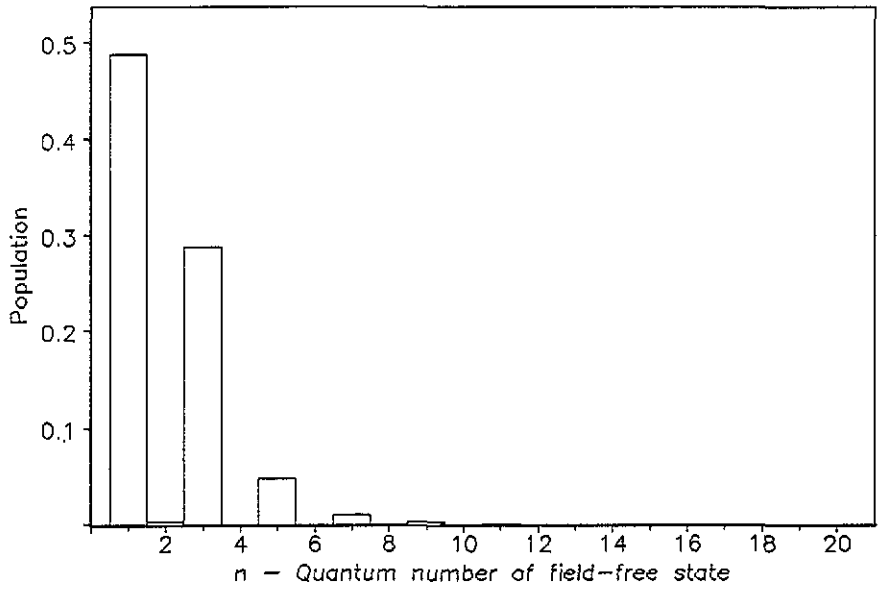

Figure 14. Field-free bound state populations at the end of the pulse used in figure 13.

The condition on $\boldsymbol{k} \cdot \boldsymbol{\alpha}$ can then be interpreted more meaningfully when the condition $\omega \gg |E_{KH}|$ is satisfied. E_{KH} is the binding energy of the atom in the electric field and when this is considerably less than ω, then an ionized electron has an outgoing wavevector that can be written as $k \approx \sqrt{2\omega}$, because the binding energy can be neglected. Examining the condition for ionization suppression parallel to the electric field, we can then write

$$k\alpha \gg 1 \qquad \sqrt{2\omega}\,\alpha \gg 1 \qquad \alpha^2\omega \gg \tfrac{1}{2} \tag{33}$$

which is comparable to Gavrila and Kaminski's condition for ionization suppression [152]. So $k \cdot \alpha \gg 1$ is a sufficient condition for ionization suppression along the axis of electric field polarization, but if $\omega \gg |E_{KH}|$ is satisfied, then Gavrila and Kaminski's original conditions are obtained.

What are the *physical* requirements for ionization suppression to occur? Perhaps the easiest to envisage is that the bound electron must predominantly 'see' the time-averaged potential, so that $V_0(\alpha_0; r)$ must be a good approximation to the actual KH frame potential. We could perhaps express this by saying that the speed of oscillation of the potential must be larger than the speed of the bound electrons' motion.

Other workers have also tried to define conditions for suppression to occur. Law *et al* have expressed the stabilization criteria in equations (30) and (31) in terms of other physical requirements [149]: ionization suppression is observable if the atom–field potential is distorted enough so that one-photon ionization can occur and the lowest two KH bound eigenstates are degenerate. Also α_0 must be greater than the width of the field-free atomic potential. They identify the onset of such suppression at a wavelength of 158 nm and intensities around 10^{16} W cm^{-2}, but at these wavelengths, the intensities that are presently available fall well short of those required.

Various workers have also tried to recast equations (30) and (31) in terms of more familiar physical quantities [159, 160]. Pont *et al* suggests that suppression can occur when the ponderomotive (oscillatory) energy of the electron is larger than the photon energy. This is put forward as a general condition for stabilization not limited to the high frequency regime. Similarly in a recent paper, Vos and Gavrila have examined which atomic states could be stabilized using lasers that are readily available today (e.g. lasers parameters of 1064 nm and 10^{14} W cm^{-2}) [161]. They identify stabilization with such lasers for atoms in high magnetic number states (and therefore high n and l states). This brings the possibility of experimentally observing super-intense stabilization much more closely. However determining the stabilization conditions becomes more complicated when an excited atom is considered. Pont and Shakeshaft have studied such cases and identify the principal quantum numbers and the orbital and magnetic quantum numbers as important in determining when ionization suppression occurs [159, 160]. The situation is complicated by centrifugal barriers and the coupling between highly excited states because of the laser bandwidth.

Other studies of stabilization have used classical techniques and have produced results that can reconfirm the conclusions from the quantum mechanical calculations [162, 163]. As yet most of the work on super-intense field ionization suppression has been theoretical, because the intensities and frrequencies we are concerned with are as yet unobtainable experimentally. To examine ground state ionization suppression, the ideal laser would have a peak intensity of at least 10^{19} W cm^{-2}, a wavelength of 10 nm and pulses of only a few femtoseconds. There are at present several possible sources of such soft x-rays that could be developed, for example the action of a strong laser field on a medium could produce very high order harmonics as mentioned above, but all the intensities yet available fall well short of what is required.

In conclusion, super-intense field ionization suppression is a phenomenon of great interest to a theorist as a testing ground for techniques not dependent on perturbation theory. Stabilization has stimulated a great deal of interest presumably because it is counter-intuitive to our concepts of strong laser fields producing rapid evolutions.

There is now general agreement that under the right conditions, ionization suppression certainly takes place, although the exact criteria are as yet unresolved and

the opportunities for further theoretical examination of Rydberg state stabilization are many. Furthermore, with rapidly increasing technology, the day is approaching when the first super-intense field ionization experiments can be performed.

Acknowledgments

We would like to thank our many colleagues who have discussed intense field physics with us over several years. This work was supported in part by the UK Science and Engineering Research Council and by the Science Plan of the European Community.

Note added in proof. High harmonics have now been observed to orders well in excess of 100 [164]. The cut-off in the harmonic order corresponds closely to that predicted by Krause *et al* [165], i.e. an XUV harmonic energy of around three times the ponderomotive shift plus the atomic ionization potential.

References

[1] Göppert-Meyer M 1931 *Ann. Phys., Lpz.* **9** 273
[2] Hughes V and Grabner L 1950 *Phys. Rev.* **79** 314
[3] Kaiser W and Garrett C G B 1961 *Phys. Rev. Lett.* **7** 229
[4] Abella I D 1963 *Phys. Rev. Lett.* **9** 453
[5] Hall, J L, Robinson E J and Branscomb L M 1965 *Phys. Rev. Lett.* **14** 1013
[6] Voronov G S and Delone N B 1966 *Sov. Phys.-JETP* **23** 54
[7] Agostini P, Barjot G, Bonnal J F, Mainfray G, Manus C and Morellec J 1968 *IEEE J. Quantum Electron* **QE-4** 667
[8] Weingartshofer A, Holmes J K, Caudle G, Clarke E M and Krüger H 1977 *Phys. Rev. Lett.* **39** 269
[9] Agostini P, Fabre F, Mainfray G, Petite G and Rahman N K 1979 *Phys. Rev. Lett.* **42** 1127
[10] Freeman R R and Bucksbaum P H 1991 *J. Phys. B: At. Mol. Opt. Phys.* **24** 325
[11] Shore B W and Knight P L 1987 *J. Phys. B: At. Mol. Phys.* **24** 325
[12] L'Huillier A, Schafer K J and Kulander K C 1991 *Phys. Rev. Lett.* **66** 2200; 1991 *J. Phys. B: At. Mol. Opt. Phys.* **24** 3315
[13] L'Huillier A, Lompré L A, Mainfray G and Manus C 1990 *Proc. 5th Int. Conf. on Multiphoton Processes*, (Paris: CEA) p 45
[14] Crane J K, Perry M D, Herman S and Falcone R W 1992 *Opt. Lett.* to be published
[15] Miyazaki K and Sakai H 1992 *J. Phys. B: At. Mol. Opt. Phys.* **25** L83
[16] Sakura N, Hata K, Adachi T, Nodomi R, Watanabe M and Watanabe S 1991 *Phys. Rev.* A **42** 1669
[17] Macklin J J, Kmetic J D, Gordon C L III and Harris S E to be published
[18] Martin E A Jr and Mandel L 1976 *Appl. Opt.* **15** 2378
[19] Boreham B W and Luther-Davies B 1979 *J. Appl. Phys.* **50** 2533
[20] Kruit P, Kimman J and van der Wiel M J 1981 *J. Phys. B: At. Mol. Phys.* **14** L597
[21] Fabre F, Petite G, Agostini P and Clement M 1982 *J. Phys. B: At. Mol. Phys.* **15** 1353
[22] Kruit P, Kimman J, Muller H G and van der Wiel M J 1983 *Phys. Rev.* A **28** 248
[23] Muller H G, Tip A and van der Wiel M J 1983 *J. Phys. B: At. Mol. Phys.* **16** L679
[24] Mittleman M H 1984 *Phys. Rev.* A **29** 2245;
Szoke A 1985 *J. Phys. B: At. Mol. Phys.* **18** L427
[25] Lompré L A, L'Huillier A, Mainfray G and Manus C 1985 *J. Opt. Soc. Am.* B **2** 1906
[26] Xiong W, Yergeau F, Chin S L and Lavigne P 1988 *J. Phys. B: At. Mol. Phys.* **21** L159
[27] Bucksbaum P H, Freeman R R, Bashkansky M and McIlrath T J 1987 *J. Opt. Soc. Am.* B **4** 760
[28] Freeman R R, McIlrath T J, Bucksbaum P H and Bashkansky M 1986 *Phys. Rev. Lett.* **57** 3156
[29] Petite G, Agostini P and Yergeau F 1987 *J. Opt. Soc. Am.* B **4** 765
[30] Freeman R R, Bucksbaum P H, Milchberg H, Darack S, Schumacher D and Geusic M E 1987 *Phys. Rev. Lett.* **59** 1092
[31] Agostini P, Antonetti A, Breger P, Crance M, Migus A, Muller H G and Petite G 1989 *J. Phys. B: At. Mol. Opt. Phys.* **22** 1971
[32] Kupersztych J, Lompré L A, Mainfray G and Manus C 1980 *J. Phys. B: At. Mol. Opt. Phys.* **21** L517

[33] Reed V C and Burnett K 1990 *Phys. Rev.* A **42** 3152; 1991 *Phys. Rev.* A **43** 6217
[34] Reed V C and Burnett K 1992 *Phys. Rev.* A **46** 424
[35] Augst S, Meyerhofer D D, Strickland D and Chin S L 1991 *J. Opt. Soc. Am.* B **8** 858
[36] Rae S C Private communication
[37] Dorr M, Feldmann D, Potvliege R M, Rottke H, Shakeshaft R, Welge K H and Wolff-Rottke B Private communication
[38] Gontier Y and Trahin M 1980 *J. Phys. B: At. Mol. Phys.* **13** 4383
[39] Pan L, Taylor K T and Clark C W 1989 *Phys. Rev.* A **39** 4894
Klarsfeld S and Maquet A 1980 *Phys. Lett.* **78A** 40
Gontier Y, Rahman N K and Trahin M 1986 *Phys. Rev.* A **34** 112; 1988 *Europhys. Lett.* **5** 595
Lambropoulos P 1988 *Multiphoton Processes* (Cambridge: Cambridge University Press) p 350
[40] Potvliege R and Shakeshaft R 1989 *Phys. Rev.* A **39** 1545
[41] Lompré L A, L'Huillier A, Mainfray G and Manus C 1985 *J. Opt. Soc. Am.* B **2** 1906
[42] Lambropoulos P 1976 *Adv. At. Mol. Phys.* **12** 87
Georges A T and Lambropoulos P 1980 *Adv. Electron. Electron. Phys.* **34** 190
[43] Eberly J H, Javanainen J and Rzazewski 1991 *Phys. Rep.* **204** 331
[44] Berson I Y 1975 *J. Phys. B: At. Mol. Phys.* **8** 3078
[45] Crance M and Aymar M 1980 *J. Phys. B: At. Mol. Phys.* **13** L421
[46] Edwards M, Pan L and Armstrong L 1984 *J. Phys. B: At. Mol. Phys.* **17** L515; 1984 *J. Phys. B: At. Mol. Phys.* **18** 1927
[47] Tang X, Lyras A and Lambropoulos P 1989 *Phys. Rev. Lett.* **63** 972
Tang X, Lambropoulos P, L'Huillier A and Dixit S N 1989 *Phys. Rev.* A **40** 7026
[48] Bialynicka-Birula Z 1984 *J. Phys. B: At. Mol. Phys.* **17** 3091
Deng Z and Eberly J H 1984 *Phys. Rev. Lett.* **53** 1810; 1985 *J. Opt. Soc. Am.* B **2** 486; 1985 *J. Phys. B: At. Mol. Phys.* **18** L287
[49] Dulčić A 1987 *Phys. Rev.* A **35** 1673
Lewenstein M, Mostowski J and Trippenbach M *J. Phys. B: At. Mol. Phys.* **18** L461
[50] Gordon W 1929 *Ann. Phys. Lpz.* **2** 1031
[51] Veniard V and Piraux B R M 1990 *Phys. Rev.* A **41** 4019
[52] Tang X, Rudolph H and Lambropoulos P 1990 *Phys. Rev. Lett.* **65** 3269;
Bachau H, Lambropoulos P and Tang X 1990 *Phys. Rev.* A **42** 5801
[53] Susskind S M and Jensen R V 1988 *Phys. Rev.* A **38** 711
[54] Sundaram B and Armstrong L Jr 1988 *Phys. Rev.* A **38** 152; 1990 *J. Opt. Soc. Am.* B **7** 414
[55] Piraux B and Knight P L 1989 *Phys. Rev.* A **40** 712
[56] Fedorov M V and Movsesian A M 1988 *J. Opt. Soc. Am.* B **5** 850; 1988 *J. Phys. B: At. Mol. Opt. Phys.* **21** L155; 1989 *J. Opt. Soc. Am.* B **6** 928; 1989 *J. Opt. Soc. Am.* B **6** 1504
Fedorov M V and Ivanov M Yu 1990 *J. Opt. Soc. Am.* B **7** 569
Fedorov M V, Ivanov M Yu and Movsesian A M 1990 *J. Phys. B: At. Mol. Phys.* **23** 2245
[57] Parker J and Stroud C R Jr 1990 *Phys. Rev.* A 1990 **41** 1602
[58] Piraux B, Huens E and Knight P L 1991 *Phys. Rev.* A **44** 721
[59] Keldysh L V 1965 *Sov. Phys.-JETP* **20** 1307
[60] Faisal F H M 1973 *J. Phys. B: At. Mol. Phys.* L89
[61] Reiss H R 1980 *Phys. Rev.* A **22** 1786
[62] Reiss H R 1987 *J. Phys. B: At. Mol. Phys.* **20** L79
[63] Reiss H R 1987 *J. Opt. Soc. Am.* B **24** 726
[64] Becker W, Schlicher R R and Scully M O 1986 *J. Phys. B: At. Mol. Phys.* **19** L785
[65] Becker W, Schlicher R R, Scully M O and Wódkiewicz K 1987 *J. Opt. Soc. Am.* B **4** 743
[66] Milonni P W 1988 *Phys. Rev.* A **38** 2682
[67] Milonni P W and Ackerhalt J R 1989 *Phys. Rev.* A **39** 1139
[68] Basile S, Ferrante G and Trombetta F 1988 *J. Phys. B: At. Mol. Opt. Phys.* **21** L377
Trombetta F, Basile S and Ferrante G *J. Phys. B: At. Mol. Opt. Phys.* **21** L539
[69] Bucksbaum P H, Freeman R R, Bashkansky M and McIlrath T J 1987 *Phys. Rev. Lett.* **58** 349
[70] Petite G, Agostini P and Muller H G 1988 *J. Phys. B: At. Mol. Opt. Phys.* **21** 4097
[71] Bashkansky M, Bucksbaum P H and Schumacher D W 1988 *J. Phys. Rev. Lett.* **60** 2458; 1988 *Phys. Rev. Lett.* **59** 274
[72] Shirley J H 1965 *Phys. Rev.* B **138** 979
[73] For example Potvlieg R M and Shakeshaft R 1988 *Phys. Rev.* A **38** 4597
[74] Chu S-I and Reinhardt W P 1977 *Phys. Rev. Lett.* **39** 1195
Chu S-I and Cooper J 1985 *Phys. Rev.* A **32** 2769
Chu S-I 1985 *Adv. At. Mol. Phys.* **21** 197
Burke P G, Francken P and Joachain C J *J. Phys. B: At. Mol. Opt. Phys.* **21** 761

[75] Potvliege R M and Shakeshaft R 1988 *Phys. Rev.* A **38** 1098; 1988 *Phys. Rev.* A **38** 6190; 1989 *Phys. Rev.* A **40** 4061
[76] Rottke H, Wolff B, Brickwedde X, Feldmann D and Welge K H 1990 *Phys. Rev. Lett.* **64** 404
[77] Burke P G, Francken P and Joachain C J 1990 *Europhys. Lett.* **13** 617; 1991 *J. Phys. B: At. Mol. Opt. Phys.* **24** 761
Dörr M, Terao-Dunseath M, Purvis J, Noble C J, Burke P G and Joachain C J 1992 *J. Phys. B: At. Mol. Opt. Phys.* **25** 2809
[78] Javanainen J, Eberly J H and Su Q 1988 *Phys. Rev.* A **38** 3430
[79] LaGattuta K J 1989 *Phys. Rev.* A **40** 683
[80] Bardsley J N Szöke A and Comella M J 1988 *J. Phys. B: At. Mol. Opt. Phys.* **21** 3899
[81] Collins L A and Merts A L 1988 *Phys. Rev.* A **37** 2415
[82] Su Q, Eberly J H and Javanainen J 1990 *Phys. Rev. Lett.* **64** 862
[83] Up to intensities where relativistic corrections need be considered, the magnetic field interaction is of the order of $a_0 ec/\mu_B \approx 300$ times smaller than the electric field interaction.
[84] Su Q and Eberly J H 1991 *Phys. Rev.* A **43** 2474
[85] Tang X and Basile S 1991 *Phys. Rev.* A **44** R1455
[86] Burnett K, Knight P L, Piraux B R M and Reed V C 1991 *Phys. Rev. Lett.* **66** 301
[87] Geltman S 1977 *J. Phys. B: At. Mol. Phys.* **10** 831
[88] Becker W, Long S and McIver J K 1990 *Phys. Rev.* A **41** 4112
[89] You L, Mostowski J and Cooper J unpublished
[90] Javanainen J and Eberly J H 1989 *Phys. Rev.* A **39** 458
[91] Pindzola M S and Dörr M 1991 *Phys. Rev.* A **43** 439
[92] Kulander K C and Shore B W 1990 *J. Opt. Soc. Am.* B **7** 502
[93] Perry M D, Szöke A and Kulander K C 1987 *Phys. Rev. Lett.* **63** 1058
[94] Kulander K C 1987 *Phys. Rev.* A **36** 2726; 1988 *Phys. Rev.* A **38** 778
[95] Kulander K C and Shore B W 1989 *Phys. Rev. Lett.* **62** 524
[96] Ferray M, L'Huillier A, Li X F, Lompré L A, Mainfray G and Manus C 1989 *J. Phys. B: At. Mol. Opt. Phys.* **21** L31
[97] Li X F, L'Huillier A, Ferray M, Lompré L A and Mainfray G 1989 *Phys. Rev.* A **39** 5751
[98] LaGattuta K J 1990 *Phys. Rev.* A **41** 5110
[99] Roso-Franco L, Sanpera A, Pons M Ll and Plaja L 1991 *Phys. Rev.* A **44** 4652
[100] DeVries P L 1980 *J. Opt. Soc. Am.* B **7** 90517
[101] Krause J L, Schafer K J and Kulander K C 1992 *Phys. Rev.* A **45** 4998
[102] Jensen R V and Sundaram B 1990 *Phys. Rev. Lett.* **65** 1964
[103] Percival I C and Richards D 1975 *Adv. At. Mol. Phys.* **11** 1
[104] Koch P M, van Leeuwen K A H, Rath O, Richards D and Jensen R V 1987 *The Physics of Phase Space* (New York: Springer) p 106
[105] For example Han C S 1990 *J. Phys. B: At. Mol. Opt. Phys.* **23** L495
[106] For example Kyrala G A 1987 *J. Opt. Soc. Am.* B **4** 731;
Grochmalicki J, Mostowski J and Trippenbach M 1988 *J. Phys. B: At. Mol. Opt. Phys.* **21** 1673
[107] For example Leopold J G and Percival I C 1978 *J. Phys. B: At. Mol. Phys.* **12** 709
Galvez E J, Sauer B E, Moorman L, Koch P M and Richards D 1988 *Phys. Rev. Lett.* **61** 2011
[108] For example Bandarage G, Maquet A and Cooper J 1990 *Phys. Rev.* A **41** 1744
[109] Grochmalicki J, Lewenstein M and Rzazewski K 1991 *Phys. Rev. Lett.* **66** 1038
[110] Sauer B E, Bellerman M R W and Koch P M 1992 *Phys. Rev. Lett.* **8** 1633
[111] Jensen R V, Sanders M M, Saraceno M and Sundaram B 1989 *Phys. Rev. Lett.* **63** 2771
[112] Bokor J, Bucksbaum P H and Freeman R R 1983 *Opt. Lett.* **8** 217
[113] McPherson A, Gibson G, Jara H, Johann U, Luk T S, McIntyre I A, Boyer K and Rhodes C K 1987 *J. Opt. Soc. Am.* B **4** 595
[114] Lompré L A, L'Huillier A, Ferray M, Monot P, Mainfray G and Manus C 1991 *J. Opt. Soc. Am.* B **7** 754
[115] L'Huillier A, Li X F and Lompré L A 1990 *J. Opt. Soc. Am.* B **7** 527
[116] Eberly J H, Su Q and Javanainen J 1989 *Phys. Rev. Lett.* **62** 881
[117] Eberly J H, Su Q and Javanainen J 1989 *J. Opt. Soc. Am.* B **6** 1289
[118] Potvliege R M and Shakeshaft R 1989 *Phys. Rev.* A **40** 3061
Potvliege R M and Shakeshaft R *J. Opt. Soc. Am.* B **7** 433
[119] Sundaram B and Milonni P W 1990 *Phys. Rev.* A **41** 6571
[120] Eberly J H, Su Q, Javanainen J, Kulander K C, Shore B W and Roso-Franco L 1989 *J. Mod. Opt.* **36** 829
[121] Shore B W 1990 *The Theory of Coherent Atomic Excitation* vol 1 (New York: Wiley) p 667
[122] Knight P L and Milonni P W 1980 *Phys. Rep.* **66** 21

[123] LaGattuta K 1992 *J. Mod. Opt.* **39** 1181
[124] For experimental results see Petite G, Agostini P and Yergeau F 1987 *J. Opt. Soc. Am.* B **4** 765
Freeman R R, Bucksbaum P H, Milchberg H, Darack S, Schumacher D and Geusic M E 1987 *Phys. Rev. Lett.* **59** 1092
[125] Becker W, Long S and McIver J K 1990 *Phys. Rev.* A **41** 4112
[126] Shore B W and Kulander K C 1989 *J. Mod. Opt.* **36** 857
[127] Shore B W and Knight P L 1987 *J. Phys. B: At. Mol. Phys.* **20** 413
[128] Ammosov M V, Delone N B and Krainov V P 1986 *Sov. Phys.-JETP* **64** 1191
Perelomov A M, Popov V S and Terent'ev M V 1965 *Sov. Phys.-JETP* **23** 924
[129] Augst S, Strickland D, Meyerhofer D D, Chin S L and Eberly J H 1989 *Phys. Rev. Lett.* **63** 2212
[130] Shih-I Chu and Yin R Y 1987 *J. Opt. Soc. Am.* B **4** 720
[131] Leopold J G and Percival I C 1979 *J. Phys. B: At. Mol. Phys.* **12** 709
[132] Bandarage G, Maquet A and Cooper J 1990 *Phys. Rev.* A **41** 1744
[133] L'Huillier A, Balcou P and Lompré L A 1992 *Phys. Rev. Lett.* **68** 166
Balcou P, Cornaggia C, Gomes A S L, Lompré L A and L'Huillier A 1992 *J. Phys. B: At. Mol. Opt. Phys.* **25** 4467
[134] Lambropoulos P 1985 *Phys. Rev. Lett.* **55** 2141
[135] Parker J and Stroud C R Jr 1980 *Phys. Rev.* A **40** 5651
[136] Cardimona D A, Raymer M G and Stroud C R Jr 1982 *J. Phys. B: At. Mol. Phys.* **15** 55
[137] Gray H R, Whitley R M and Stroud C R Jr 1982 *Opt. Lett.* **3** 218
Radmore P M and Knight P L 1982 U39 **15** 561
Coleman P E and Knight P L 1982 *J. Phys. B: At. Mol. Phys.* **15** L235
[138] Alber G and Zoller P 1988 *Phys. Rev.* A **37** 377
Alber G, Haslwanter Th and Zoller P 1988 *J. Opt. Soc. Am.* B **5** 2439
[139] Alber G, Ritsch H and Zoller P 1986 *Phys. Rev.* A **34** 1058
[140] Yeazell J A, Mallalieu M and Stroud C R Jr 1990 *Phys. Rev. Lett.* **64** 2007
[141] Burnett K, Reed V C, Cooper J and Knight P L 1992 *Phys. Rev.* A **45** 3349
[142] Jones R R and Bucksbaum P H 1991 *Phys. Rev. Lett.* **67** 3215
[143] Noordam L D, Stapelfeldt H, Duncan D I and Gallagher T F 1992 *Phys. Rev. Lett.* **68** 1496
[144] Pont M, Walet N R, Gavrila M and McCurdy C W 1988 *Phys. Rev. Lett.* **61** 939
For example Eberly J H, Grobe R, Law C K and Gavrila M 1992 *Atoms in Intense Laser Fields* ed M Gavrila (Boston: Academic)
[145] Pont M and Gavrila M 1990 *Phys. Rev. Lett.* **65** 2362
[146] Reed V C, Knight P L and Burnett K 1991 *Phys. Rev. Lett.* **67** 1415
[147] Kulander K C, Schafer K J and Krause J L 1991 *Phys. Rev. Lett.* **66** 2601
[148] Reiss H 1992 *Phys. Rev.* A **46** 391
[149] Law C K, Su Q and Eberly J H 1991 *Phys. Rev.* A **44** 7844
[150] Kramers H A 1956 *Collected Scientific Papers* (Amsterdam: North-Holland) p 866
[151] Henneberger W C 1868 *Phys. Rev. Lett.* **21** 838
[152] Gavrila M and Kaminski J Z 1984 *Phys. Rev. Lett.* **52** 613
Offerhaus M J, Kaminski J Z and Gavrila M 1985 *Phys. Lett.* **112A** 151
Gavrila M, Offerhaus M J and Kaminski J Z 1986 *Phys. Lett.* **118A** 331
van de Ree J, Kaminski J Z and Gavrila M 1988 *Phys. Rev.* A **37** 4536
[153] Pont M, Walet N R and Gavrila M 1990 *Phys. Rev.* A **41** 477
[154] Pont M 1989 *Phys. Rev.* A **40** 5659
[155] Reed V C, Burnett K and Knight P L *Phys. Rev.* A submitted
Reed V C 1992 *Mod. Phys. Lett.* **6** 683
[156] Su Q and Javanainen J 1990 *J. Opt. Soc. Am.* B **7** 564
[157] Leopold J G and Percival I C 1978 *Phys. Rev. Lett.* **41** 944
[158] Mainfray G and Manus C 1991 *Rep. Prog. Phys.* **54** 1333
[159] Pont M and Shakeshaft R 1991 *Phys. Rev.* A **44** R4110
[160] Pont M, Proulx D and Shakeshaft R 1991 *Phys. Rev.* A **44** 4486
[161] Vos R J and Gavrila M 1992 *Phys. Rev. Lett.* **68** 170
[162] Jensen R V and Sundaram B *Phys. Rev. Lett.* submitted
[163] Richards D *J. Phys. B: At. Mol. Opt. Phys.* submitted
Benvenuto F, Casati G and Shepelyansky D L 1992 *Phys. Rev.* A **45** R7670
[164] Macklin J J, Kmetic J D and Gordon C L III 1933 to be published
L'Huillier A and Balcou P 1933 to be published
Smith R, Tisch J, Ciarocca M and Hutchinson M H R 1993 to be published
[165] Krause J L, Schafer K J and Kulander K C 1992 *Phys. Rev. Lett.* **68** 3535